

THESIS

GEOLOGY OF THE ALICE E. BRECCIA
PIPE AND VICINITY, NEW WORLD MINING
DISTRICT, PARK COUNTY, MONTANA

Submitted by

Edward L. Cope

Department of Earth Resources

In partial fulfillment of the requirements

for the Degree of Master of Science

Colorado State University

Fort Collins, Colorado

Summer, 1984

COLORADO STATE UNIVERSITY

Summer, 1984

WE HEREBY RECOMMEND THAT THE THESIS PREPARED UNDER OUR SUPERVISION BY EDWARD L. COPE ENTITLED GEOLOGY OF THE ALICE E. BRECCIA PIPE AND VICINITY, NEW WORLD MINING DISTRICT, PARK COUNTY, MONTANA BE ACCEPTED AS FUL-FILLING IN PART REQUIREMENTS FOR THE DEGREE OF MASTER OF SCIENCE.

Committee on Graduate Work

Larry K. Burns

D.R. Winder

Tommy B. Thompson
Adviser

A.S. Boyne
Department Head

ABSTRACT OF THESIS

GEOLOGY OF THE ALICE E. BRECCIA PIPE AND VICINITY, NEW WORLD MINING DISTRICT, PARK COUNTY, MONTANA

The Alice E. breccia pipe occurs in a one square mile area of the New World mining district, Park County, Montana. Porphyry gold type mineralization-alteration is exposed at many prospects within the study area.

Rocks exposed in the vicinity of the breccia pipe consist of Precambrian granite-gneiss, Cambrian sedimentary rocks and Tertiary subvolcanic intrusives.

Hydrothermal alteration is widespread throughout the study area. Propylitic, phyllic, and hydrous skarn alteration all occur in the breccia pipe and the rocks in the vicinity of the pipe. The alteration is zoned vertically and laterally about the breccia. Supergene alteration has resulted from the oxidation of pyritic ores enriching gold relative to other metals at the Alice E. mine.

Mineralization consisting of vein and replacement types occurs in association with the hydrothermally altered areas. Magnetite, pyrite, chalcopyrite, bornite and sphalerite occur in order of formation. Gold has accompanied the sulfide stage mineralization.

Fluid inclusion data indicate that the metals were deposited in veins whose minimum temperatures of formation ranged from 320°C to 447°C within the study area. Boiling occurred in the deepest parts of

the exposed system with metals being deposited in and above the zone of boiling. The fluids were highly saline as evidenced by the presence of halite bearing fluid inclusions.

The metals were carried in solution as chloride complexes which became unstable at temperatures less than 400°C. Metal paragenesis and zonation within the area can be explained in terms of chloride complexing and cooling of the ore solutions.

The pipe contains a collapse breccia that has been modified by the later intrusions of quartz amphibole latite porphyry dikes and a hypothetical stock which intrude the breccia pipe. The mineral deposits of the area are probably related to these intrusions.

Edward L. Cope
Department of Earth Resources
Colorado State University
Fort Collins, CO 80521
Summer, 1984

ACKNOWLEDGEMENTS

The author is indebted to Mr. Joseph J. Kapler who, while district geologist with Energy Reserves Group, suggested the thesis project and provided employment and research funding. Special thanks are extended to Dr. Tommy B. Thompson for his assistance and guidance in the laboratory studies and his constructive criticism during the project. The author is also indebted to Mr. Harold J. Prostka and Mr. James E. Elliott who provided data and helpful discussions of the geology of the study area. Appreciation is extended to Dr. D. Winder of the Department of Physics for serving on the thesis committee.

Very special thanks are extended to the relatives and friends who helped by providing encouragement throughout the project.

TABLE OF CONTENTS

	<u>Page</u>
INTRODUCTION	1
Location and Access	1
Geography	1
Climate	4
Vegetation	4
History.	6
Previous Work	6
Purpose and Methods of Investigation	7
REGIONAL GEOLOGY	9
Beartooth Uplift	9
Absaroka Volcanic Field	10
Tectonic Implications	11
GEOLOGY OF BRECCIA PIPE AND VICINITY	14
Precambrian Rocks	14
Granite Gneiss	14
Cambrian Sedimentary Rocks	17
Flathead Sandstone	17
Wolsey Shale	19
Meagher Limestone	20
Park Shale	20
Pilgrim Limestone	20
Tertiary Igneous Rocks	22
Trachyandesite Porphyry Sill	24
Diorite Sill	27
Rhyodacite Porphyry	27
Biotite Latite Porphyry Stock	31
Quartz Amphibole Latite Porphyry	35
Latite Porphyry	38
Quartz Latite Porphyry	43
Breccia Pipe.	46
Quaternary Deposits	46
Glacial Deposits	46
Undifferentiated Alluvium	46
PETROGENESIS	48
STRUCTURE	54
Faults	54
Veins and Dikes	54
Sheet and Stockwork Fracturing	55

TABLE OF CONTENTS (Cont'd)

	<u>Page</u>
HYDROTHERMAL ALTERATION	57
Propylitic Alteration	57
Phyllic Alteration	58
Hydrous Skarn Alteration	59
SUPERGENE ALTERATION	68
MINERALIZATION	69
Vein Mineralization	69
Skarn-Replacement Mineralization	72
Paragenesis	75
FLUID INCLUSIONS	83
Types of Inclusions	83
Two Phase Liquid Dominated Inclusions	86
Gas Rich Inclusions	86
Halite-Bearing Inclusions	86
Homogenization Temperatures	87
Salinity	89
GEOCHEMISTRY	92
Gold	92
Silver	93
Copper	93
Molybdenum	94
Zinc	94
Lead	94
Cu-Mo-Au Relationship	95
DISCUSSION	97
Breccia Pipe Genesis	97
Controls of Mineralization	98
Physical Controls	98
Chemical Controls	99
CONCLUSION AND RECOMMENDATION FOR FURTHER EXPLORATION	102
REFERENCES CITED	104

TABLE OF CONTENTS (Cont'd)

	<u>Page</u>
APPENDIX	109
Semi-Quantative Method of Determining Quartz Contents of Porphyritic-Aphanitic Rocks Using X-Ray Diffraction	113
Introduction	113
Sample Preparation	113
Preparation of Standard Samples	113
X-Ray Procedure	114
Assimilation of Data	114

LIST OF TABLES

<u>Table</u>		<u>Page</u>
1	Modal analysis (volume percent) for rhyodacite porphyry sill	31
2	Modal analyses (volume percent) for biotite latite porphyry	32
3	Modal analyses (volume percent) for three quartz amphibole latite samples	38
4	Modal analysis (volume percent) of latite porphyry	40
5	Modal analysis (volume percent) for quartz latite porphyry	43
6	Fluid inclusion data obtained from heating stage study.	88
7	Geochemical data for 55 Alice E. samples	110
8	Quartz, orthoclase and oligoclase contents of synthetic rock standards	114
9	Data obtained by measuring the area under the 60° 2θ quartz peaks from X-ray diffraction patterns	115
10	Weight percent quartz for three Alice E. samples . . .	115
11	Heating stage data for primary fluid inclusions in quartz related to sulfide-gold mineralization at the Alice E. mine and vicinity	118

LIST OF FIGURES

<u>Figure</u>		<u>Page</u>
1	Topographic map of the New World Mining District	2
2	View of the southern end of Henderson Mountain looking west	3
3	Geographic features of the Beartooth-Absaroka-Yellowstone region	5
4	Sample of granite gneiss stained for potassium feldspar	16
5	Photomicrograph of sample CC-82-6 crossed nicols)	16
6	Cut specimen of Flathead Sandstone (Cf), sample CC-82-61	18
7	Cut sample of shale fragment from breccia pipe material, sample CC-82-34	21
8	Classification diagram for volcanic rocks using quartz, alkali feldspar, plagioclase modal data	23
9	Specimen of trachyandesite porphyry (Ttp) stained for potassium feldspar identification	26
10	Photomicrograph of trachyandesite porphyry (sample CC-82-51) (crossed nicols)	26
11	Photomicrograph of diorite (Td) (crossed nicols)	28
12	Cut specimen of rhyodacite porphyry (Trp), stained for potassium feldspar	30
13	Photomicrograph of rhyodacite porphyry, sample CC-82-68 (crossed nicols)	30
14	Cut specimen of biotite latite porphyry (Tb1p), stained for potassium feldspar	34

LIST OF FIGURES (Cont'd)

<u>Figure</u>		<u>Page</u>
15	Photomicrograph of biotite latite porphyry, sample CC-82-9 (crossed nicols)	34
16	Cut specimen of quartz amphibole latite porphyry (Tqalp), stained for potassium feldspar	37
17	Photomicrograph of quartz amphibole latite porphyry, sample CC-82-44 (crossed nicols)	37
18	Photomicrograph of quartz amphibole latite porphyry (Tqalp), sample CC-82-45 (crossed nicols)	39
19	Cut specimen of latite porphyry (Tlp), stained for potassium feldspar	42
20	This section photomicrograph of latite porphyry, sample CC-82-55 (crossed nicols)	42
21	Cut specimen of quartz latite porphyry (Tqlp), stained for potassium feldspar	45
22	Photomicrograph of quartz latite porphyry, sample CC-82-65 (crossed nicols)	45
23	Cut specimen of breccia pipe material (Tbx)	47
24	Diagram depicting the evolution of the intrusive rocks of the Alice E. vicinity.	49
25	Harker variation diagram for K_2O-SiO_2	51
26	Cut specimen of phyllic altered dike rock	61
27	Cut specimen of altered quartz amphibole latite porphyry	61
28	Photograph showing contact between quartz amphibole latite porphyry and breccia pipe material	64
29	Photomicrograph of sample CC-82-29 (crossed nicols)	64
30	Cut specimen of breccia pipe material (Tbx)	66
31	Photomicrograph of sample CC-82-53 (crossed nicols)	66

LIST OF FIGURES (Cont'd)

<u>Figure</u>		<u>Page</u>
32	Photograph of sheet fractured zone at the Alice E. mine	71
33	Closeup of sheet fractures in sandstone at the location in Figure 32.	71
34	Cut specimen of Wolsey Shale (Cw) replaced by magnetite and pyrite	74
35	Polished section photomicrograph of sample CC-82-50 (plane reflected light)	74
36	Paragenetic diagram for mineralization at the Alice E. mine and vicinity	76
37	Polished section photomicrograph of sample CC-82-52 (plane reflected light)	77
38	Polished section photomicrograph of sample CC-82-33 (plane reflected light)	80
39	Polished section photomicrograph of sample CC-82-35 (plane reflected light)	80
40	Polished section photomicrograph of sample CC-82-52 (plane reflected light)	82
41	Polished section photomicrograph of sample CC-82-30 (plane reflected light)	82
42	Sketches of fluid inclusion types observed in Alice E. vein and open space breccia filling quartz	85
43	Polished plate photomicrograph of sample CC-82-53 (plane light)	85
44	T-X projection in the system NaCl-H ₂ O	90
45	Plot of compositional data for 55 Alice E. samples	96
46	Graphic representation of X-ray diffraction data	116

LIST OF PLATES

<u>Plate</u>		<u>Page</u>
1	Geologic map of the Alice E. breccia pipe and vicinity	In pocket
2	Alteration-mineralization map of the breccia pipe and vicinity	In pocket
3	Cross-section of the Alice E. breccia pipe	In pocket

INTRODUCTION

Location and Access

The Alice E. prospect is located in sec. 24, T. 9 S, R. 14 E, within the south central portion of the New World Mining District, Park County, Montana (Fig. 1). The main workings of the Alice E. mine are approximately centered in sec. 24, on the south slope of Henderson Mountain (Fig. 2), about one mile north of Cooke City. Cooke City is four miles east of the northeast entrance to Yellowstone National Park, on U.S. Highway 12.

Travel to Cooke City is on the highway through Yellowstone Park from Gardner, Montana and from Cody, Wyoming and Red Lodge, Montana. Access to the prospect area is via the unmaintained forest service road that leaves the Beartooth Highway about one half mile east of Cooke City. This road follows Miller Creek up Henderson Mountain to Daisy Pass.

The Gardiner-Yellowstone route is the only year-round access since the Beartooth Highway is not maintained during the winter and spring months.

Geography

The New World District is within the Central Rocky Mountain province, between the Beartooth Mountains to the north and the Absaroka Mountains to the south. The Yellowstone Plateau and the

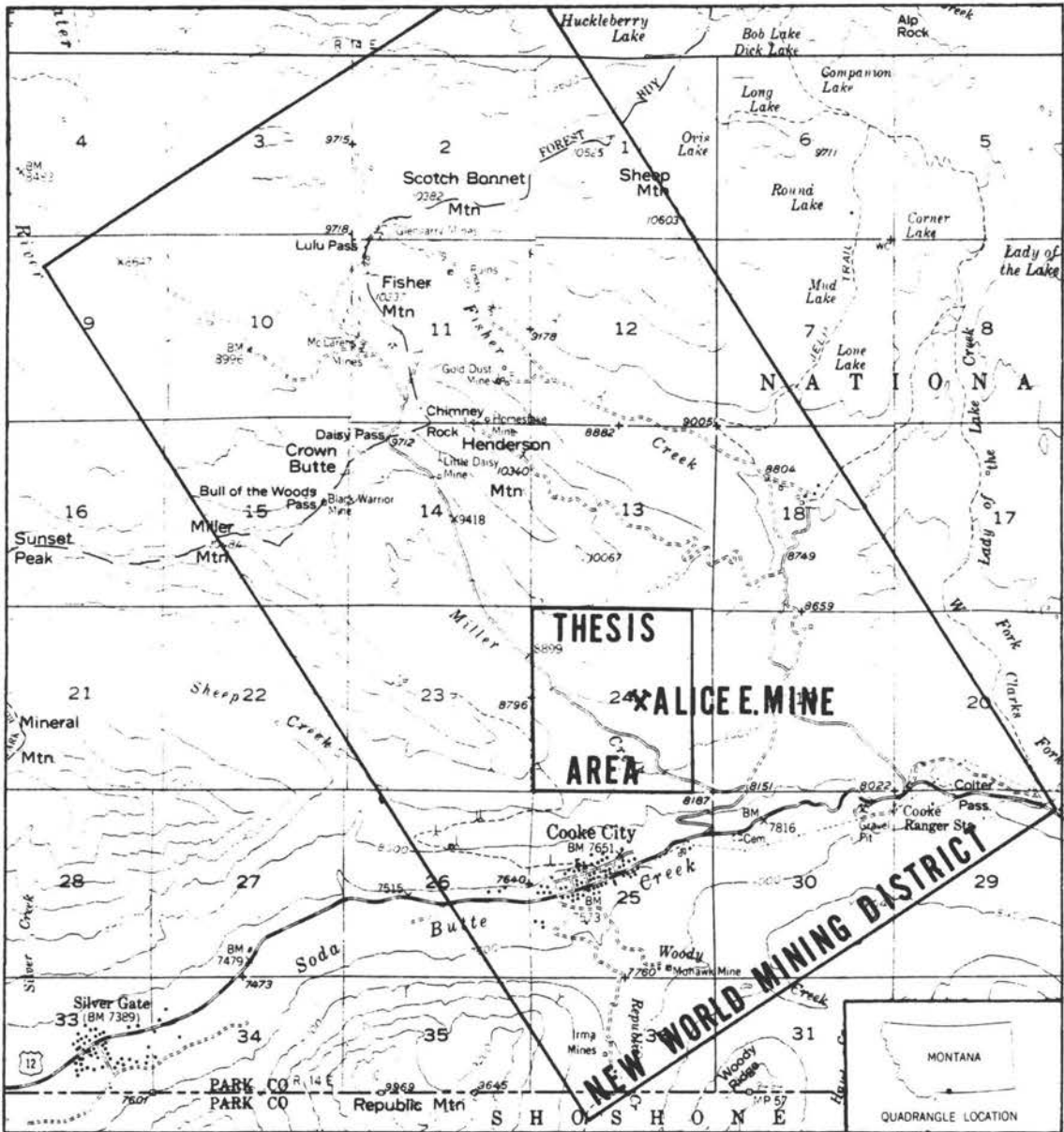


Figure 1. Topographic map of the New World Mining District. Map shows the location of the thesis area and the Alice E. gold mine. Adapted from U.S.G.S. Cooke City, Montana, 15 minute quadrangle.

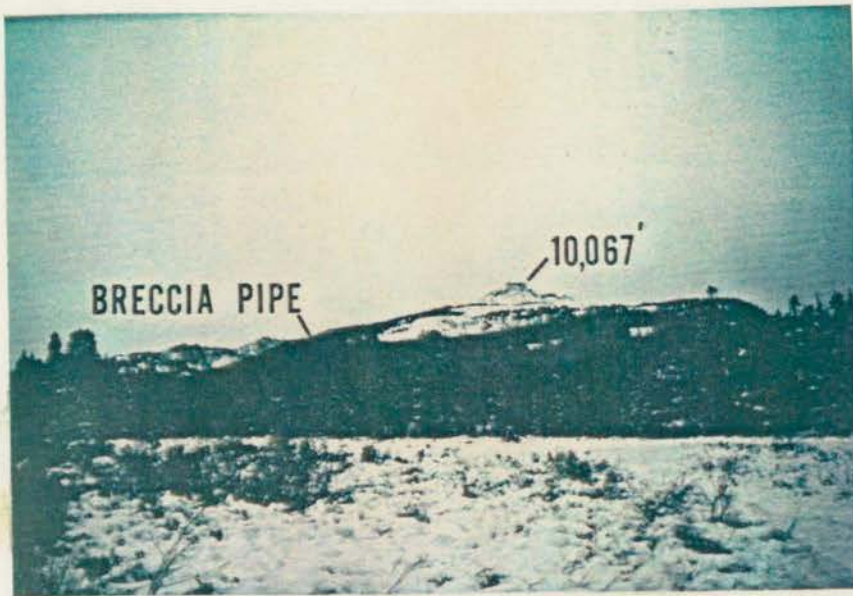


Figure 2. View of the southern end of Henderson Mountain looking west. Highest point is 10,067 feet elevation. Note location of breccia pipe which shows weak topographic expression in the photo.

Snowy Mountains lie to the southwest and northwest, respectively (Fig. 3). The elevation within the area ranges from 8,600 feet to 9,600 feet above sea level. The highest elevation on Henderson Mountain is 10,340.

Glacial deposits are common in the map area. These deposits were formed during the Pleistocene by glaciers in Miller Creek and Fisher Creek.

Climate

The climate in the area is as would be expected for a sub-alpine environment at 45 degrees north latitude. Precipitation averages about 20 inches to 30 inches per year with about 250 inches to 350 inches of snow annually. Snow may occur in any month of the year and usually covers the ground from November to June. Deep snow drifts last well into July and many of the peaks retain some snow throughout the entire year.

During the 1982 field season, the first heavy snowfall occurred on September 12th and by early October the field season was over due to snow.

The summers are short and cool in this alpine region.

Vegetation

Vegetation within the thesis area vary from dense stands of pine, fir and spruce at the lower elevations to scrub pine and juniper at the higher elevations. Within the dense portions of the forest, deadfall is a hindrance to mapping. The northwest part of sec. 24 is just at the treeline on Henderson Mountain.

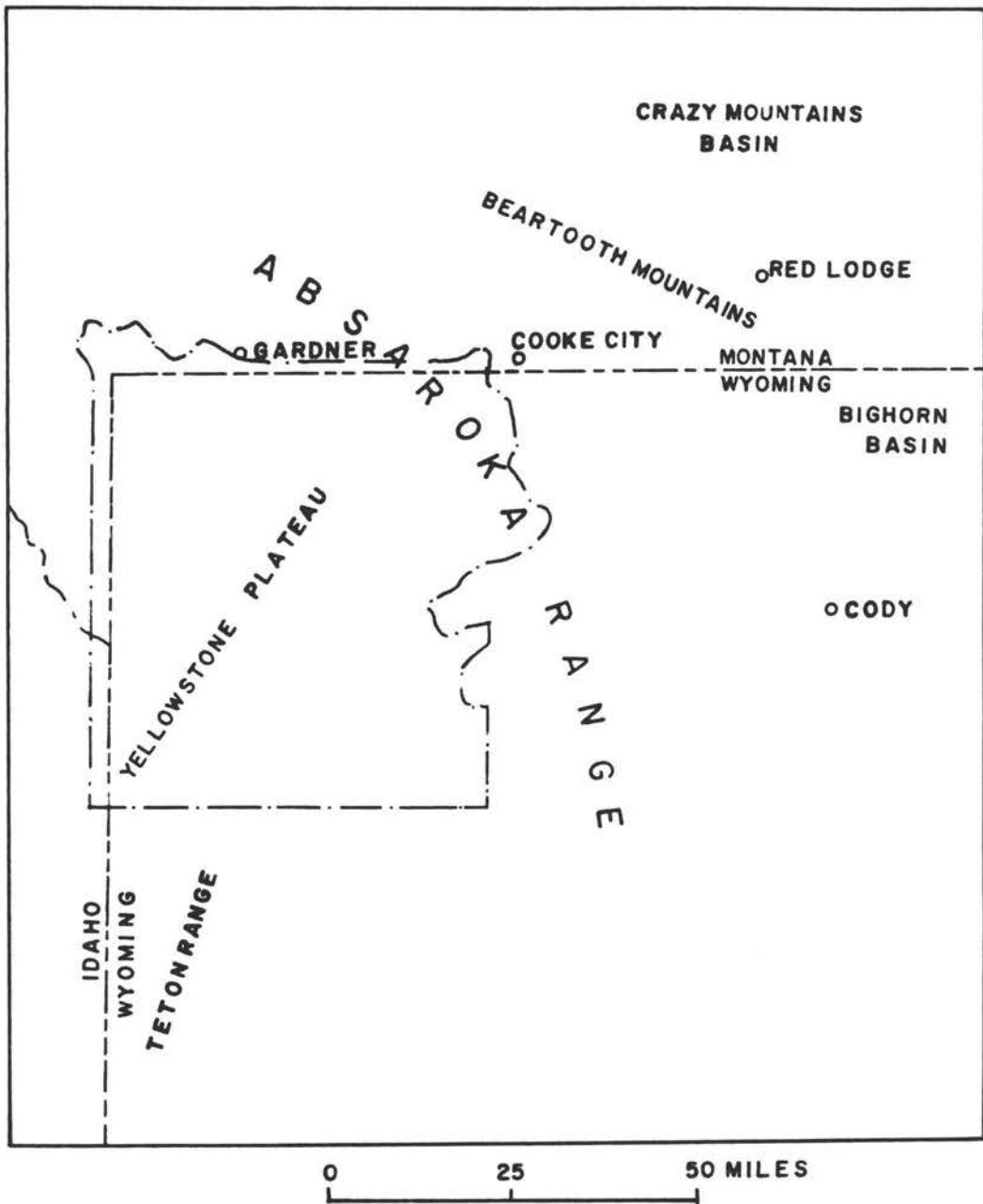


Figure 3. Geographic features of the Beartooth-Absaroka-Yellowstone region. Adapted from Smedes and Prostka (1972).

History

Gold was discovered at the Alice E. about 1893. By 1895 approximately 2,500 tons of gold ore averaging 0.7 ounces/ton had been mined and treated (Reed, 1950). According to Reed, the ore was treated in a cyanide plant near the mine. The operations were suspended when increasing sulfides were encountered not far from the surface. The oxidized part of the ore body was amenable to leaching but the pyritic ores were not.

The workings consist of a small open cut and numerous adits, shafts and prospect pits. All of the underground workings have been inaccessible at least since Lovering (1929) visited the property.

Workings have been developed on a number of patented claims in the vicinity of the Alice E. Production from these workings is unknown, but is assumed to be minor judging by the size of the dumps at these prospects.

The cyanide mill foundation and a few collapsed cabins are all that remain from the early mining days at the Alice E.

Previous Work

Numerous papers have been published on the New World Mining District. Lovering (1929) completed the first modern detailed study of the district.

Reed (1950) described the mineral occurrences of Park County. In this paper he discusses the major mines and prospects of the New World Mining District.

Recent studies on the geology of the district include three master's theses and one doctoral dissertation.

Jansons (1963) studied the petrology and trace element geochemistry of the Henderson Mountain porphyry.

The Irma-Republic mines at the south end of the district were studied by Butler (1965).

Horrall (1966) provided a detailed petrologic description of the Henderson Mountain intrusive.

The economic geology of the district was studied by Eyrich (1969) as part of his doctoral work. This study deals with the northern and central portions of the district. The Alice E. was not discussed in any detail in the dissertation.

Elliott (1979) mapped the southwest corner of the Cooke City 15 minute quadrangle at a scale of 1:24,000.

The Alice E. mine is discussed by Lovering (1929), and Reed (1950) provided a crude sketch map of the mine area with a brief description of the mine geology.

The mapping by Elliott (1979) was the first published material to demonstrate that the Alice E. mine occurs within a large Tertiary breccia pipe. His description of the breccia is as follows

Explosion-collapse (?) breccia consisting of fragments of mostly Pilgrim Limestone, Park Shale and Wolsey Shale in a pulverized rock-flour matrix, locally strongly altered and mineralized, intruded by dikes of weakly altered, light colored quartz latite porphyry. This porphyry contains abundant phenocrysts of rounded quartz, pale-green to colorless clinopyroxene and or amphibolite, plagioclase and sparse large potassium feldspars in an aphanitic potassium feldspar-rich groundmass.

Purpose and Methods of Investigation

This thesis is the culmination of research funded in part by Energy Reserves Group Inc. The project was intended to investigate

the occurrence and potential of low grade gold mineralization localized in and adjacent to felsic porphyritic plutons. Early in the study the association between alkaline porphyritic plutons and gold mineralization was recognized. The term "porphyry gold" has been applied to the genetic model that was developed (Cope, 1981). Breccia pipes and linear breccia bodies were found to be integral features often associated with mineralization.

In 1981 a field program was initiated to evaluate the gold mining districts within the alkalic igneous province of central Montana. The author mapped and sampled many prospects in the alkalic belt as defined by Lange (1977).

Gold mineralization was recognized at the Alice E. late in the summer of 1981 and plans were made to continue the study in 1982.

Field work for this study was completed late in the summer of 1982. The Alice E. breccia pipe and vicinity were mapped at a scale of 1:2,400 (Plates 1, 2 and 3). Samples were collected for laboratory and geochemical analysis.

Laboratory work consisted of thin section and polished section studies of the igneous rocks and ore specimens. Doubly polished plates were prepared for fluid inclusion analysis. Stained slabs (Bailey and Stevens, 1960) were used to study the textural and mineralogic character of the igneous rocks. Many samples were scanned by X-ray diffraction methods to aid in mineral identification.

REGIONAL GEOLOGY

The Beartooth uplift and the Absaroka volcanic field are the main geologic features of the region. A brief summary of the structural and tectonic setting of northwestern Wyoming and southwestern Montana, during the late Mesozoic and early Cenozoic eras, is necessary to explain the course of events resulting in magmatic and hydrothermal activity in the New World Mining District.

Beartooth Uplift

The Beartooth uplift is a roughly rectangular block of dominantly Precambrian Archean crystalline rocks. It is composed primarily of granite gneiss, amphibolite, minor quartzites, and iron formation intruded by mafic dikes (Foose and others, 1961). The gneissic rocks are dated at 2,750 m.y. and the younger mafic dikes are dated at 2,500 m.y. (Elliott, 1979) in the Cooke City area.

The Beartooth uplift exists today as a largely denuded block of crystalline rocks bounded by high angle normal faults and rather steeply dipping thrust faults. The block is surrounded by the Bighorn Basin, the Nye-Bowler zone, the Crazy Mountains Basin and the Absaroka-Yellowstone volcanic area.

Foose and others (1961) discuss the structural geology of the block, and identify the Mill Creek-Stillwater zone and the Cooke City zone as the important lineaments or structural zones affecting the

block. The Cooke City zone has played an important role in localizing intrusions in the New World District.

They describe the Cooke City zone as being a trough-like depression, cutting across the block in a northwest direction. Cambrian sediments are preserved along much of the Cooke City zone. The strata commonly dip towards the center of the depression in synclinal fashion. Fractures within the zone generally trend northwest and parallel many of the Precambrian mafic dikes (Foose and others, 1961). The zone has localized Laramide and Tertiary igneous intrusions. Volcanic vent and ring dike complexes remain today as eroded remnants of former volcanoes.

Absaroka Volcanic Field

The Absaroka volcanic field covers 9,000 square miles in northwestern Wyoming and southwestern Montana.

The field consists largely of andesitic volcanoclastic rocks that have been subdivided into three groups comprising the Absaroka Volcanic Supergroup (Smedes and Prostka, 1972). The groups are named in decreasing order of age: (1) Washburn Group; (2) Sunlight Group; (3) Thorofare Creek Group. These replace the terminology introduced by Hague (1899) (Early basic breccia), that was widely used until recently (Lovering, 1929; Rouse, 1937; Parsons, 1939; Eyrich, 1969).

Calc-alkalic andesites and dacites make up 90 percent of the Absaroka volcanic rocks. The remaining 10 percent of the field is composed of potassic rocks of the shoshonite suite (Lipman and others, 1972). Absaroka volcanics are remarkably similar to

circum-pacific andesites in Indonesia, New Guinea, Fiji and Kamchatka. The areas mentioned all contain shoshonitic lavas and intrusive equivalents.

The term shoshonite was applied to rocks of the Absaroka-Yellowstone region by Iddings (1895). Recent studies have delved into the formation of these highly potassic rocks (Joplin, 1964; Prostka, 1972). Prostka (1972) suggests that a hybrid origin for shoshonite is evident from petrographic and trace element data.

The Absaroka volcanic rocks were erupted from numerous vent complexes that are aligned along two main parallel eruptive belts known as the eastern and western intrusive belts (Chadwick, 1970). Chemical analyses show that the eastern belt of intrusives is enriched in K_2O when compared to the western belt. The Cooke City intrusive complex lies within the eastern, K_2O -enriched intrusive belt.

Intrusive rocks of these belts consist of diorite, andesite, quartz-monzonite, syenogabbro and syenite (Parsons, 1939; Lovering, 1929). The eruptive centers are variable in size and nature and generally include stocks, sills, and laccoliths with ring dikes, radial dikes, and breccia pipes, often with associated sulfide mineralization.

The New World Mining District is roughly centered over one of these vent complexes. It is a major stock with laccoliths, sills and three large breccia pipes. Sulfide mineralization accompanied development of the vent complex.

Tectonic Implications

It is not possible to relate the geology of the study area to continental tectonics, however, it is clear that uplift and volcanism in the

region occurred during the Laramide Orogeny, and continued into Eocene time.

Compilation of age dates and chemical data for late Cretaceous and early Tertiary volcanic fields of the western United States show that volcanic processes can repeatedly be related to subduction and arc magmatism (Lipman, 1980).

The geologic history of the Beartooth-Absaroka region shows that a dramatic transformation began about 80 m.y. ago and has continued into recent time, with periodic lulls in activity. The sequence of events during the late Cretaceous and early Tertiary are presented below, highlighting the current plate tectonic theories.

During the interval 80-70 m.y. ago arc magmatism moved eastward from Idaho into Montana (Lipman, 1980). The Elkhorn volcanics were erupted contemporaneously with the intrusion of the Boulder batholith at this time. Magmatic activity ceased about 70 m.y. ago with the lull lasting until 60 m.y. ago.

The interval 60-50 m.y. was probably the most important in the development of the Beartooth uplift. Increased rates of subduction and significant flattening of the dip of the subducted plate are proposed for this time (Dickenson, 1979). Compressive forces due to crustal shortening resulting from this type of subduction easily explain uplifting of the Beartooth and other mountain ranges of the central Rocky Mountains. The Absaroka volcanic activity commenced during this time span.

Magmatic activity started abruptly about 50 m.y. ago in much of Idaho, western and central Montana, and northwestern Wyoming. Uplifting and adjustment of the Beartooth block continued. The

greatest volume of Absaroka volcanic rocks was erupted shortly after 49 m.y. ago (Smedes and Prostka, 1972). The youngest igneous rocks are not dated but it is probable that most of the late igneous activity related to Absaroka volcanism occurred no later than about 40 m.y. ago.

Figure 1. Spectra of quartz and calcite extracted from the sample 00-85. The quartz (q) and calcite (c) are the dominant minerals. The spectra are shown in the figure. The quartz (q) and calcite (c) are the dominant minerals. The spectra are shown in the figure.

Figure 2. X-ray diffraction patterns of sample 00-85. The quartz (q) and calcite (c) are the dominant minerals. The spectra are shown in the figure. The quartz (q) and calcite (c) are the dominant minerals. The spectra are shown in the figure.

Figure 4. Sample of granite gneiss stained for potassium feldspar. Specimen contains potassium feldspar (yellow), quartz (gray), altered feldspar (white). Silica flooding occurs adjacent to quartz-sulfide veinlet.

Figure 5. Photomicrograph of sample CC-82-6 (crossed nicols). Quartz (q) and microcline (m) are the dominant minerals. Weak sericite and calcite alteration is present.

GEOLOGY OF BRECCIA PIPE AND VICINITY

Precambrian Rocks

Granite Gneiss (Wg)

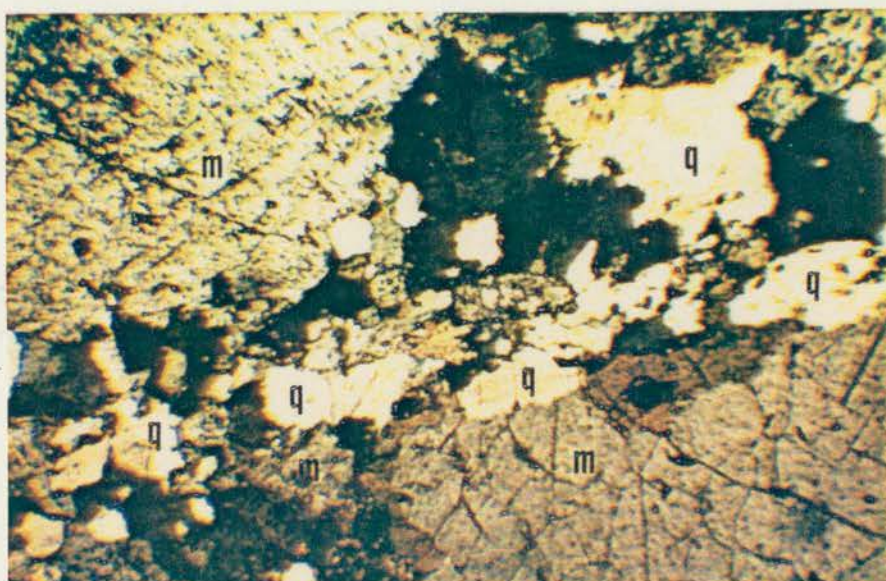
Precambrian granitic rocks crop out at a number of localities in the thesis study area (Plate 1). Unaltered samples of the granite are medium grained, equigranular, often weakly to moderately foliated.

The granite gneiss is composed primarily of quartz (35%) and microcline (50%) plus sericite (15%). Stained slabs (Fig. 4) demonstrate the textural and mineralogic nature of a typical sample. All of the samples collected in the vicinity were altered significantly making accurate modal analysis difficult. The composition is in agreement with Eyrich's (1969) analysis of fresh samples assuming all albite and minor mafic minerals (hornblende, biotite) in Alice E. samples have been altered to sericite.

Petrographic and X-ray diffraction studies confirm the hand specimen analysis. The bulk of the granites examined contained quartz and potassium feldspar with quartz, sericite and sulfides as alteration products of feldspars and mafic minerals (Fig. 5). Highly altered specimens are composed of quartz and sericite with carbonate.

Quartz flooding and quartz-carbonate-sulfide veinlets are observed invading the granite in strongly altered-mineralized zones.

Secondary fluid inclusions of several types are common in primary quartz crystals.



0.2 mm

Cambrian Sedimentary Rocks

Cambrian sedimentary rocks are preserved along much of the Cooke City structural zone. Sedimentation was initiated in Middle Cambrian time upon a gently undulating erosion surface of minor relief that had developed on the Precambrian basement complex (Eyrich, 1969). Eyrich (1969) estimated that 1,100 feet of Middle and Upper Cambrian sediments are exposed in the New World District.

Elliott's (1979) map of the district shows that approximately 680 feet of Middle and Upper Cambrian sedimentary rocks occur in sec. 24 at the southwest corner of the map area (Plate 1). The geologic map shows the sedimentary rocks as they were drawn on the map by Elliot (1979) with the appropriate scale adjustment.

The Cambrian sedimentary rocks have been carefully studied by Eyrich (1969). Much of the material that follows is summarized from this work.

Flathead Sandstone (Cf)

The Flathead Sandstone is a medium bedded basal sandstone deposited unconformably on the Precambrian basement complex. The thickness is variable due to minor relief on the Precambrian surface (Eyrich, 1969). Most workers estimate the thickness to be about 100 feet (Eyrich, 1969; Elliott, 1979).

The formation is exposed at the Alice E. and in the northwest corner of the map area where it and Precambrian granite are intruded by a Tertiary subvolcanic porphyry pluton.

The beds are reddish brown (Fig. 6) except in areas of intense alteration and sulfide mineralization. The dominant mineral is quartz



Figure 6. Cut specimen of Flathead Sandstone (Cf), sample CC-82-61. Note presence of hematite and pyrite. This sample is from the upper part of the Formation.

with hematite and glauconite becoming important constituents in the upper portions (Eyrich, 1969). In altered zones the rocks are bleached and often contain pyrite in various stages of oxidation. Pyrite is common and is probably related to intrusive and later hydrothermal activity in the area.

The upper contact of the Flathead Sandstone is gradational with the conformably overlying Wolsey Shale. A distinct contact is difficult to establish. The sedimentary rocks surrounding much of the breccia pipe are of the transition units between the Flathead Sandstone and the Wolsey Shale.

Wolsey Shale (Cw)

The Wolsey Shale conformably overlies the Flathead Sandstone. Outcrops are rare, however samples from prospect pits are often greenish-brown when not severely altered and mineralized. Most examples from the study area contained considerable pyrite.

Eyrich (1969) describes the Wolsey Shale from drill cores. The rock is a fine grained sandstone with an argillaceous matrix in the lower part of the formation. The middle of the formation is dominated by shale which grades into thin calcareous, sandy beds at the top of the formation. Total thickness is about 180 feet.

Sills intrude the Wolsey Shale in the study area. The shale often shows contact metamorphism in areas intruded by the sills. The thin bedded calcareous beds at the top are more susceptible to the contact metamorphic effects. A banded hornfels is often the product of this metamorphism.

Meagher Limestone (€m)

The Meagher Limestone conformably overlies the Wolsey Shale. The formation is a thin bedded carbonate rock with wavy bedding planes (Eyrich, 1969). The rock type does not crop out in the northern portion of the study area. Elliott (1979) mapped a complete section of Meagher Limestone in the southwest corner of Section 24 (Plate 1).

Eyrich (1969) states that the limestone is a thin bedded (1/4 inch to 3 inches), fossiliferous micrite with oncolites at the base. Argillaceous and dolomitic interbeds occur throughout. The dolomitization is attributed to post-depositional diagenetic processes.

The formation is approximately 180 feet thick.

Park Shale (€p)

The Park Shale is conformable with the Meagher Limestone. It is a thin bedded shaly carbonate rock. Unaltered outcrops are scarce, but breccia fragments of the rock are common in the Alice E. breccia (Fig. 7). Contact metamorphic textures and minerals are present in the breccia fragments. The metamorphism probably occurred during the intrusion of Tertiary sills. Brecciation and mineralization are post-metamorphic in age at the Alice E.

The Park Shale is 250 feet thick (Eyrich, 1969; Elliott, 1979).

Pilgrim Limestone (€pi)

The Pilgrim Limestone occurs in the extreme southwest corner of the study area. Elliott (1979) describes the rock as limestone and limestone pebble conglomerate, thick bedded, approximately 250 feet



Figure 7. Cut sample of shale fragment from breccia pipe material, sample CC-82-34. Shale is Park Shale Formation showing pre-breccia metamorphic texture and later open space breccia texture with calcite infilling.

thick. The formation is the uppermost Cambrian sedimentary rock exposed in the study area.

The formation is oolitic with calcite and dolomite as major components of the limestone. It is not readily altered according to Eyrich (1969).

Tertiary Igneous Rocks

Subvolcanic intrusive rocks of Paleocene and Eocene age occur as stocks, sills, and dikes within the area. The Alice E. breccia pipe is probably Eocene in age. It is intimately related to the Tertiary igneous activity, and is described with other Tertiary igneous units.

The intrusions are observed as concordant and discordant bodies of variable composition that intrude Precambrian and Cambrian age rocks in the study area.

The porphyritic igneous rocks were difficult to study under the microscope due to the large quantity of aphanitic groundmass present in the samples.

Stained specimens were found to be the most useful in determining mineral percentages. This and the use of X-ray diffraction scans of powdered light mineral separates from the porphyritic rocks were used in estimating modal composition for porphyritic rocks. The method is described in detail in the appendix.

The porphyries were classified using the ternary Q-A-P diagram prepared by the I.U.G.S. Subcommittee for classification of volcanic rocks (Fig. 8).

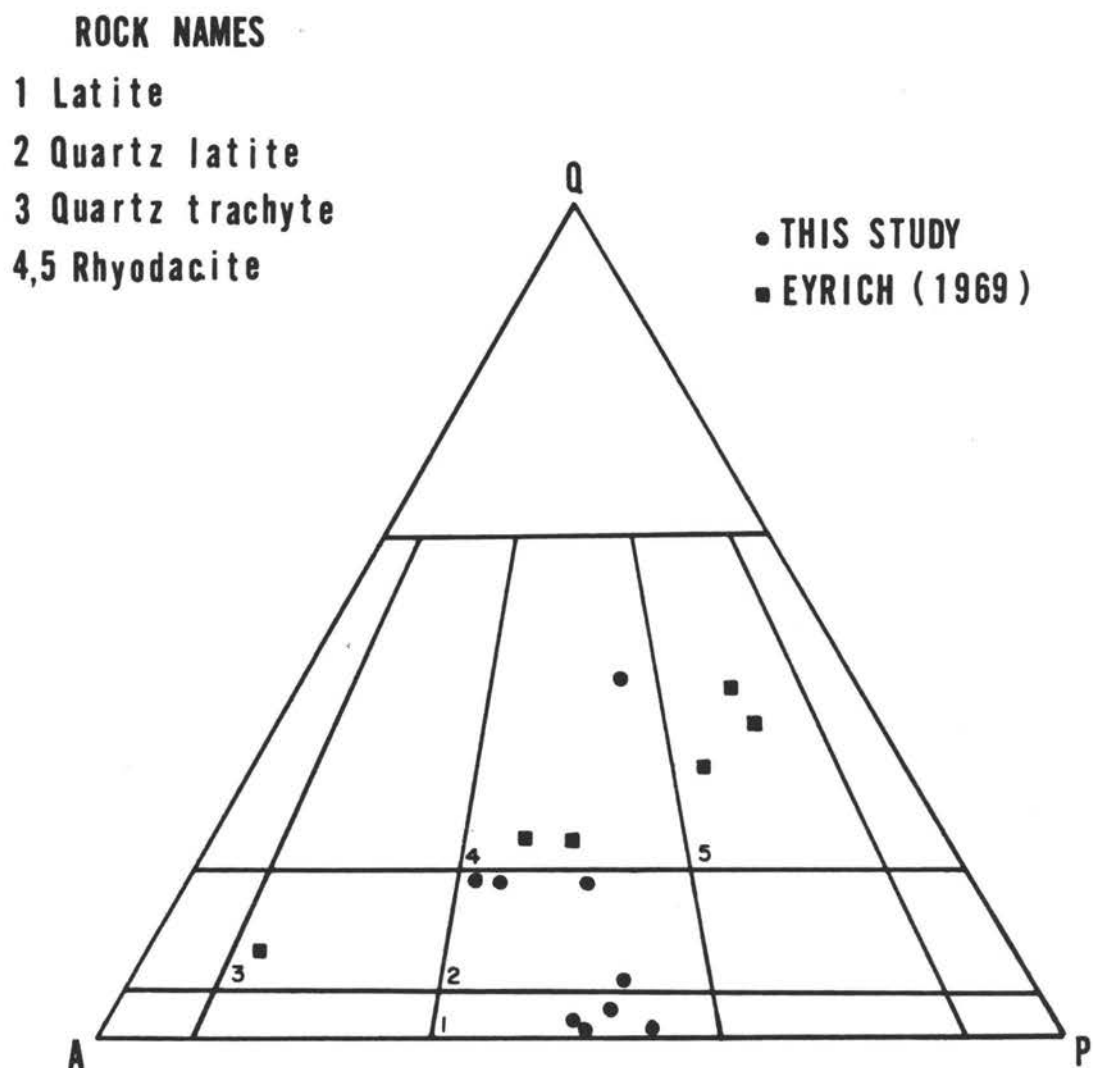


Figure 8. Classification diagram for volcanic rocks using quartz, alkali feldspar, plagioclase modal data. After Streck-eisen (1979).

Volcanic terminology is more appropriate than plutonic terminology when discussing the porphyries, due to their textural nature and subvolcanic association.

Data from Eyrich (1969) and this study are plotted on the Q-A-P diagram to compare rock compositions according to the now widely used I.U.G.S. scheme.

The plot demonstrates the variation in composition in individual and segregated igneous bodies. This is a characteristic exhibited in many epizonal intrusives of subvolcanic origin.

The rocks consist of diorite, andesite, latite, dacite, rhyodacite, quartz latite and quartz trachyte.

Trachyandesite Porphyry Sill (Ttp)

The oldest Tertiary igneous rock in the study area is a sill of light green to gray trachyandesite porphyry. The rock consists of plagioclase phenocrysts (20%), in a fine grained groundmass. The rock is commonly pyritized and is altered to propylitic and sericitic mineral assemblages. Stained slabs confirm the hand specimen mineral identification (Fig. 9).

Microscopic examination of the porphyry reveals phenocrysts of plagioclase, hornblende, and biotite in order of abundance (Fig. 10). Phenocrysts are set in a fine grained trachytic textured groundmass composed of plagioclase, with minor potassium feldspar and quartz.

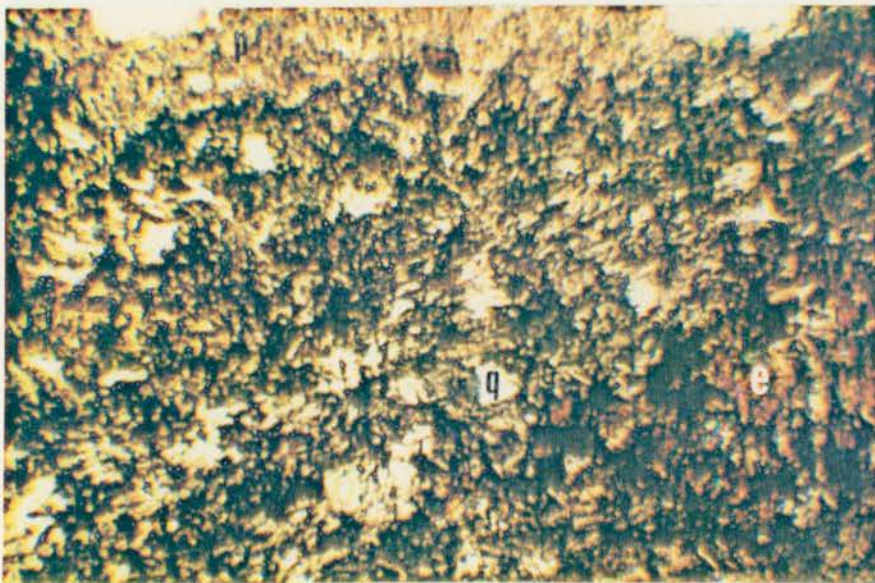
Plagioclase is commonly altered to carbonate and epidote. Hornblende is altered to epidote and biotite is altered to chlorite.

The first part of the paper is devoted to the study of the asymptotic behavior of the solutions of the system (1) as $t \rightarrow \infty$. It is shown that the solutions of the system (1) tend to zero as $t \rightarrow \infty$ if and only if the matrix A is stable.

In the second part of the paper, the problem of the asymptotic stability of the solutions of the system (1) is considered. It is shown that the system (1) is asymptotically stable if and only if the matrix A is stable and the matrix B is nonsingular.

Figure 9. Specimen of trachyandesite porphyry (Ttp) stained for potassium feldspar identification. Yellow colored areas not properly etched by HF. Sample is propylitic altered with disseminated pyrite.

Figure 10. Photomicrograph of trachyandesite porphyry (sample CC-82-51) (crossed nicols). Present are plagioclase (p); epidote (e) replacing hornblende. The groundmass is fine grained with trachytic texture. Minor secondary quartz (q) also present.



0.2 mm

Diorite Sill (Td)

A sill-like body of diorite is exposed in the southern half of the study area. Hand samples of the rock are dark gray colored and appear weakly to moderately altered. The diorite is much more strongly altered than the hand samples would suggest. It consists dominantly of plagioclase altered to an assemblage of quartz, sericite, carbonate, and pyrite. Aggregates of secondary quartz and pyrite with interstitial sericite and carbonate are a common alteration texture.

Estimates of mineral percentages are difficult due to the severity of alteration. The name is given to the rock based on Elliott's (1979) descriptions of fresh samples (Fig. 11) which are diorite to monzo-diorite in composition.

Elliott (1979) reports the date of this rock at 55.3 ± 7 m.y. The age was determined by the potassium-argon method on biotite.

Rhyodacite Porphyry (Trp)

This rock occurs as sills of light colored porphyry containing conspicuous, rounded (resorbed) phenocrysts of quartz and phenocrysts of plagioclase, hornblende, and biotite in an aphanitic groundmass of potassium feldspar and quartz (Fig. 12).

Petrographic examination (Fig. 13) confirms the phenocryst mineralogy of plagioclase (oligoclase), quartz, hornblende and biotite in order of abundance and totaling about 30 percent of the rock. The groundmass of potassium feldspar and quartz is aphanitic (<0.01 mm).

Modal analysis of a sample of the rhyodacite porphyry is presented in Table 1.



0.2mm

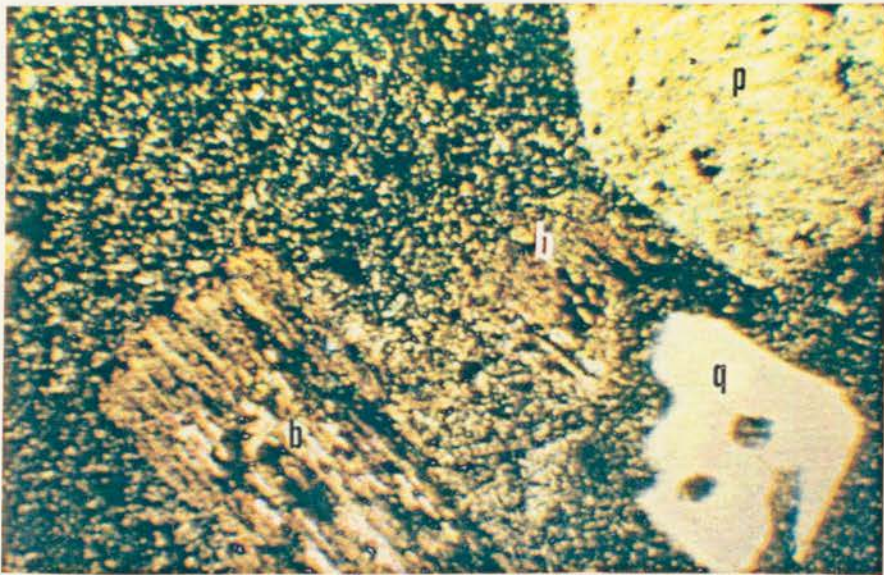
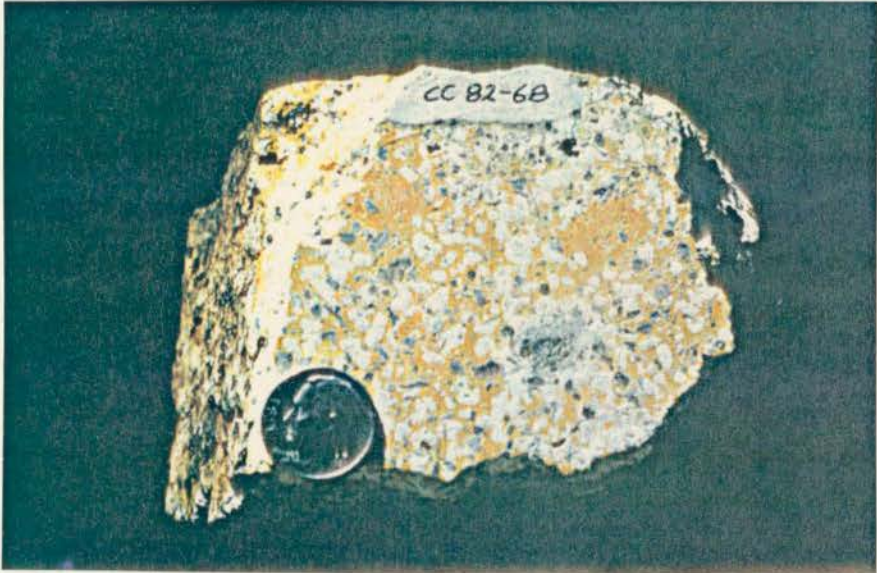
Figure 11. Photomicrograph of diorite (Td) (crossed nicols). Plagioclase (p), biotite (b), and hornblende (h) are present in order of abundance. Sample K-008B courtesy of James E. Elliott, U.S.G.S., Denver, CO.

The first part of the paper is devoted to the construction of a
 \mathbb{Z} -module structure on the space of n -tuples of
 elements of \mathbb{Z} . This is done by defining a multiplication
 operation on the set of n -tuples. The second part of the
 paper is devoted to the study of the properties of this
 multiplication operation.

The first part of the paper is devoted to the construction of a
 \mathbb{Z} -module structure on the space of n -tuples of
 elements of \mathbb{Z} . This is done by defining a multiplication
 operation on the set of n -tuples. The second part of the
 paper is devoted to the study of the properties of this
 multiplication operation.

Figure 12. Cut specimen of rhyodacite porphyry (Trp), stained for potassium feldspar. Note plagioclase (white, and quartz (gray) phenocrysts in groundmass rich in orthoclase (yellow). Minor mafic minerals as phenocrysts and in clots surrounded by plagioclase.

Figure 13. Photomicrograph of rhyodacite porphyry, sample CC-82-68 (crossed nicols). Phenocrysts are oligoclase (p), quartz (q), and biotite (b). Groundmass is orthoclase and quartz. Note resorbtion of quartz phenocryst.



0.2 mm

Table 1. Modal analysis (volume percent) for rhyodacite porphyry sill.

	Sample CC-82-68
Quartz	37
Orthoclase	22
Oligoclase	31
Hornblende	65
Biotite	4
Other	<1

This is equivalent to the quartz "eye" rhyodacite porphyry of Elliott (1979).

Quartz phenocrysts are strongly resorbed and often embayed by groundmass material. Numerous fluid inclusions are present in the quartz phenocrysts.

Plagioclase phenocrysts are euhedral to moderately rounded as a result of resorption. They are often altered to epidote, carbonate and sericite.

Euhedral to subhedral hornblende and biotite phenocrysts are weakly to moderately replaced by chlorite.

The porphyry is dated at 40.6 ± 3.5 m.y. using fission track data from zircons (Elliott, 1979).

Biotite Latite Porphyry Stock (Tb1p)

This porphyry, named "Henderson Mountain Porphyry" by previous workers (Horall, 1966; Eyrich, 1969; Elliott, 1979), is the

most massive intrusive body in the New World Mining District. The porphyry occupies much of the northern portion of the thesis area (Plate 1).

Hand samples of the rock are orange colored and contain phenocrysts of plagioclase, biotite and hornblende in an aphanitic groundmass. The porphyry is altered at all but a few locations in the study area. The stained samples of biotite latite porphyry are similar to other porphyries of the area showing a potassium felspar-rich groundmass (Fig. 14).

Microscopic study of the porphyry shows the porphyritic aphanitic texture (Fig. 15). All phenocrysts combined make up approximately 50 percent of the porphyry.

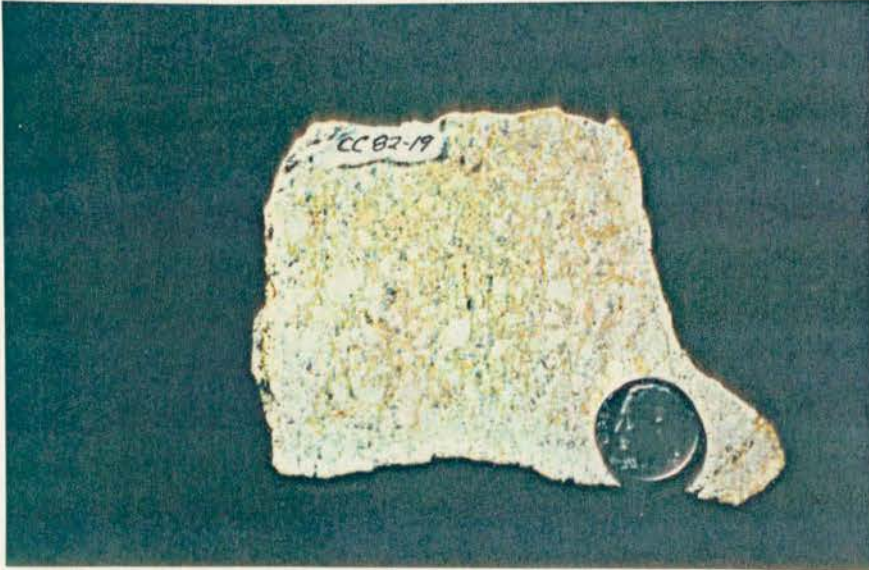
Modal analyses of three samples of biotite latite porphyry are presented in Table 2.

Table 2. Modal analyses (volume percent) for biotite latite porphyry.

	Sample		
	CC-82-9	CC-82-19	CC-82-38
Oligoclase	45	44	45
Orthoclase	42	38	44
Biotite	8	9	4
Hornblende	4	6	3
Quartz	1	3	2
Other	tr.	tr.	1

Figure 14. Cut specimen of biotite latite porphyry (Tb1p), stained for potassium feldspar. Plagioclase (white), and orthoclase (yellow) are the main minerals. Biotite and hornblende are common.

Figure 15. Photomicrograph of biotite latite porphyry, sample CC-82-9 (crossed nicols). Phenocrysts are oligoclase (p), biotite (b), and hornblende (h). Quartz content is less than 3 percent in this rock. Ground-mass is dominated by orthoclase with minor quartz.



0.2 mm

The lack of quartz in these rocks is evident in stained hand samples, thin sections and the powder X-ray data obtained.

The porphyry is altered to sericitic and propylitic types of alteration in the thesis area. This alteration is the result of late magmatic-deuteric and later hydrothermal events in the vicinity of the Alice E. mine.

Quartz Amphibole Latite Porphyry (Tqalp)

Dikes of quartz latite porphyry intrude the breccia pipe in a crude radial pattern (Plate 1). The dikes cut the breccia, the breccia-wall rock contact and continue out into the wall rocks surrounding the breccia at one locality. A crescent shaped intrusive of quartz latite porphyry cuts the breccia and biotite latite porphyry at the northwest corner of the breccia pipe. One dike cuts biotite latite porphyry near the northeast corner of the breccia pipe. The porphyry is apparently related to the breccia pipe and mineralization within it. The importance of these intrusive bodies will be addressed later.

Megascopically the dikes are light gray to green colored and consist of phenocrysts of quartz (resorbed), plagioclase, and hornblende in an aphanitic groundmass. Visible epidote gives the green color often observed.

Staining for potassium feldspar in cut samples (Fig. 16) shows plagioclase, quartz, amphibole and occasional orthoclase phenocrysts in a potassium feldspar groundmass. Fine grained sulfides were observed in the groundmass.

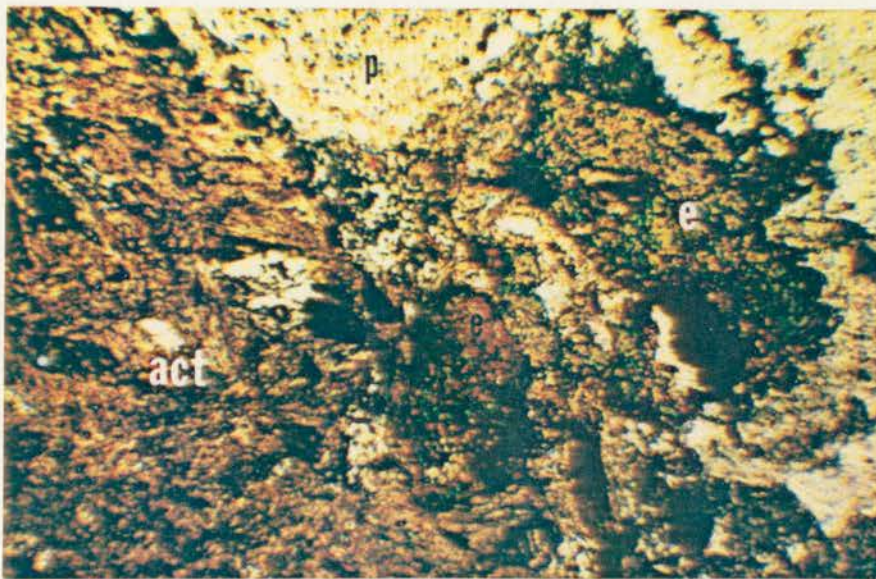
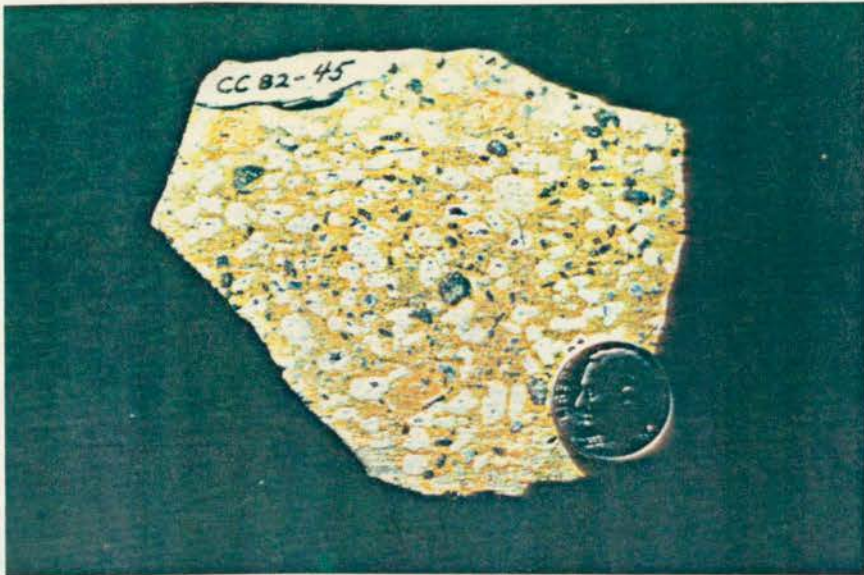
Thin sections reveal the presence of clinopyroxene (augite) in many of the samples. The pyroxene is often altered to amphibole (uralite) (Fig. 17). Plagioclase (oligoclase) is euhedral to subrounded.

The following is a list of the names of the persons who have been appointed to the various positions in the Department of the Interior, and the date of their appointment.

The following is a list of the names of the persons who have been appointed to the various positions in the Department of the Interior, and the date of their appointment.

Figure 16. Cut specimen of quartz amphibole latite porphyry (Tqalp), stained for potassium feldspar. Phenocrysts are plagioclase (white), quartz (gray), orthoclase (yellow) and hornblende-actinolite (dark green). Groundmass is dominated by orthoclase (yellow).

Figure 17. Photomicrograph of quartz amphibole latite porphyry, sample CC-82-44 (crossed nicols). Shown is uralitic replacement of hornblende and augite by actinolite (act). Epidote (e) occurs with actinolite as alteration of plagioclase and hornblende.



0.2 mm

The calcic cores of some phenocrysts are altered to epidote. Quartz phenocrysts are strongly resorbed and often invaded by the groundmass (Fig. 18).

Modal analyses for quartz amphibole latite porphyries are presented in Table 3.

Table 3. Modal analyses (volume percent) for three quartz amphibole latite samples.

	Sample		
	CC-82-32	CC-82-45	CC-82-46
Quartz	18	17	18
Orthoclase	38	38	46
Oligoclase	40	34	29
Amphibole	3	7	5
Clinopyroxene	1	2	2
Other	-	2	-

The variation of plagioclase and orthoclase is due to local differences in groundmass to phenocryst ratios.

Latite Porphyry (Tlp)

Latite porphyry dikes occur at two localities in the study area. One dike intrudes the breccia pipe just north of the main Alice E. workings (Plate 1). The other dike fills an arcuate structure possibly related to the breccia pipe. This dike is exposed in Miller Creek only.

Hand samples of the rock are green to dark gray. Plagioclase and large potassium feldspar phenocrysts are present. Biotite and



0.2 mm

Figure 18. Photomicrograph of quartz amphibole latite porphyry (Tqalp), sample CC-82-45 (crossed nicols). Depicts intense resorption of quartz phenocryst (q), in potassium feldspar-rich groundmass. Fresh hornblende present in upper right part and in center of quartz phenocryst.

hornblende phenocrysts are plentiful in the rock. Stained slabs document this mineralogy (Fig. 19). The groundmass of this porphyry is not as enriched in potassium feldspar as the porphyries previously discussed.

Petrographic examination shows the porphyritic, weakly trachytic texture present in the rock (Fig. 20). Large potassium feldspar (orthoclase) phenocrysts commonly have poikilitic intergrowths of biotite. Hornblende and biotite phenocrysts are euhedral. The lack of alteration in these dikes suggests that they are post-mineral in age. Intrusives discussed earlier are apparently pre- and inter-mineral in age.

Phenocrysts make up 40 percent of the rock. Modal analysis for one sample of latite porphyry is presented in Table 4.

Table 4. Modal analysis (volume percent) of latite porphyry.

	Sample CC-82-55
Plagioclase	50
Orthoclase	35
Biotite	9
Hornblende	5
Quartz	1

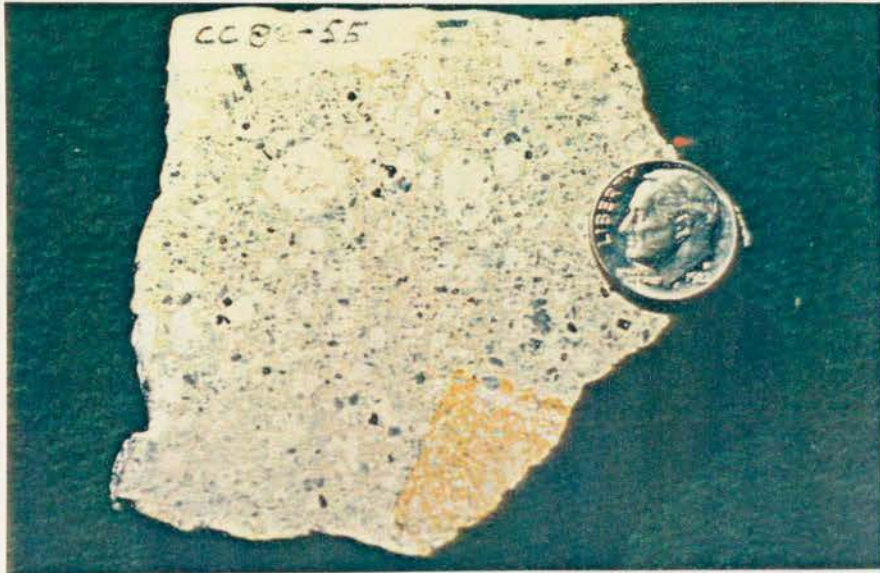
The groundmass is composed of plagioclase, potassium feldspar and quartz in order of abundance.

The first part of the paper is devoted to the study of the asymptotic behavior of the solutions of the system (1) as $t \rightarrow \infty$. It is shown that the solutions of the system (1) tend to zero as $t \rightarrow \infty$ if and only if the matrix A is stable.

The second part of the paper is devoted to the study of the asymptotic behavior of the solutions of the system (1) as $t \rightarrow \infty$. It is shown that the solutions of the system (1) tend to zero as $t \rightarrow \infty$ if and only if the matrix A is stable.

Figure 19. Cut specimen of latite porphyry (Tlp), stained for potassium feldspar. Phenocrysts are plagioclase (white), biotite (black) and orthoclase (yellow). Groundmass is orthoclase and plagioclase.

Figure 20. This section photomicrograph of latite porphyry, sample CC-82-55 (crossed nicols). Note phenocrysts of oligoclase (p), and biotite (b) in fine grained weakly trachytic groundmass. Minor hornblende (h) is altered to epidote.



0.2 mm

Quartz Latite Porphyry (Tqlp)

A late dike of quartz latite porphyry crops out in Miller Creek. This dike is arcuate and roughly parallel to the latite porphyry dike discussed in the previous rock description.

The dike is gray colored with phenocrysts of quartz, plagioclase, and orthoclase. The phenocrysts are about 50 percent of the total rock. Aphanitic groundmass makes up the remainder.

The stained specimen shows phenocryst mineralogy and texture (Fig. 21).

Modal analysis of the dike is presented in Table 5.

Table 5. Modal analysis (volume percent) for quartz latite porphyry.

	Sample CC-82-65
Oligoclase	45
Orthoclase	37
Quartz	6
Biotite	7
Hornblende	4
Other	1

The thin section of this dike shows little alteration as in other late dikes. Poikilitic textures are observed in orthoclase phenocrysts (Fig. 22).

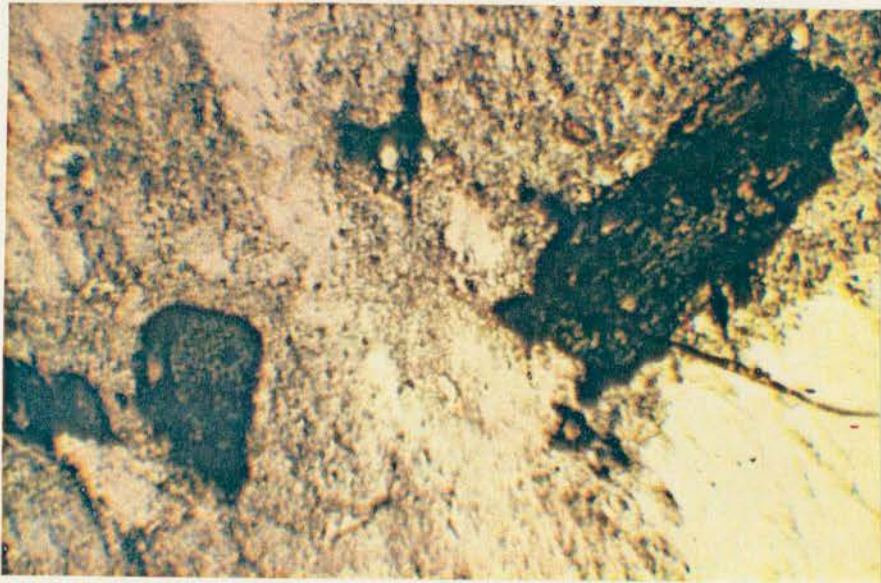
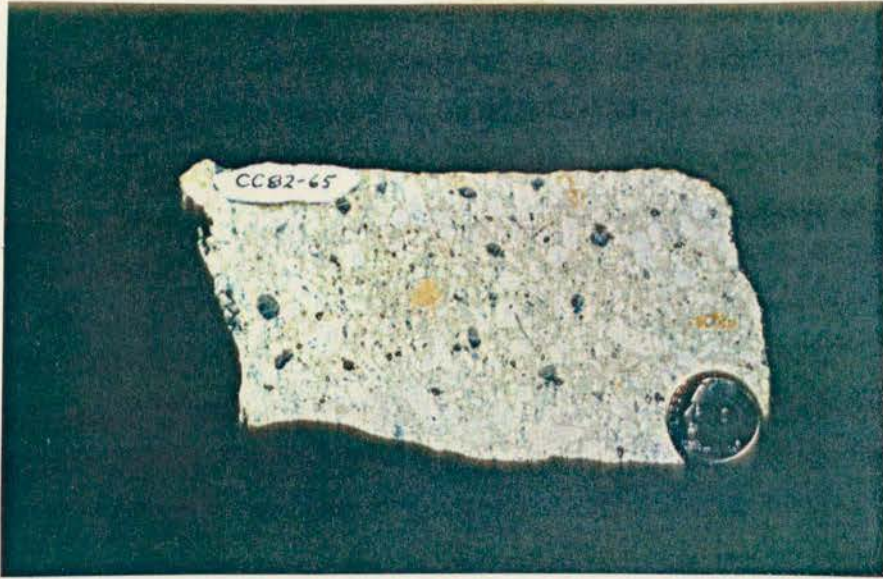
This dike was the last igneous rock to intrude the Alice E. mine area.

Figure 51. Correlation of quartz lattice porphyry (QLP) and
 quartz for potassium feldspar. The correlation in
 quartz (white), quartz feldspar, and quartz
 (yellow). Quartz was in potassium feldspar.

Figure 52. Relationship of quartz lattice porphyry, quartz
 (QLP) (white) and quartz feldspar (yellow) and
 quartz in quartz of quartz feldspar in a large
 quartz feldspar.

Figure 21. Cut specimen of quartz latite porphyry (Tqlp), stained for potassium feldspar. Phenocrysts are plagioclase (white), quartz (gray), and orthoclase (yellow). Groundmass is potassium feldspar rich.

Figure 22. Photomicrograph of quartz latite porphyry, sample CC-82-65 (crossed nicols). Highlighted are poikilitic inclusions of altered biotite in a large orthoclase phenocryst.



0.1mm

Breccia Pipe (Tbx)

The breccia body is a crescent-shaped structure that is centered in section 24. The breccia consists of dominantly Cambrian sedimentary fragments. Flathead Sandstone, Wolsey Shale and Park Shale fragments and blocks are most common. Meagher Limestone and Pilgrim Limestone fragments are poorly represented and are assumed to have been replaced by post-breccia hydrothermal minerals. Trachyandesite porphyry fragments were noted at one location. Diorite blocks (?) are present near the southern contact of the breccia and diorite.

The fragments are angular with weak to moderate fragment rotation exhibited in the samples collected (Fig. 23). The fragments are cemented by products that post-date the brecciation event. Calcite, quartz, epidote, actinolite, and adularia are noted cementing breccia fragments.

The genesis of this breccia pipe and the mineralized zones within it are presented later in the discussion, following descriptions of the alteration and mineralization.

Quaternary Deposits

Glacial Deposits (Qg)

Glacial deposits occur on the eastern and western flanks of the southern end of Henderson mountain. The deposits are mentioned because they represent an obstacle to geologic and geochemical surveys.

Undifferentiated Alluvium (Qu)

The slopes of Henderson mountain are covered by much debris. Colluvium is well developed on gentle to moderately steep terrain. Talus occupies the lower portions of the steeper slopes.



Figure 23. Cut specimen of breccia pipe material (Tbx). Angular fragments of Park Shale are cemented by late calcite with base metals (sphalerite, chalcopryite).

PETROGENESIS

The evolution of the Cooke City intrusive complex can be traced by studying the change in composition of progressively younger intrusive bodies.

Age dates and field relationships show that the oldest intrusives of the complex are dioritic (andesitic) in composition. The diorite of Scotch Bonnet mountain is dated at 55.3 ± 0.7 m.y. ago (Elliott, 1979). The diorite body in the study area is probably the same age according to Elliott. Andesitic border phases occur at the contacts of these intrusives (Eyrich, 1969). Paleocene andesitic dikes are also present in the Cooke City area (Elliott, 1979).

Evidence suggests that these early intrusions are closely related to andesitic volcanic rocks that were erupted during Paleocene time. Prostka (personal comm., 1982) has postulated that the Cathedral Cliffs Formation volcanics were erupted from vents in the Cooke City area. The diorite and andesite intrusions coincide with the eruption of andesitic volcanoclastics of the Cathedral Cliffs Formation. Following extrusion of the volcanics, the vents were plugged with the diorite bodies, and differentiation of the remaining magma began.

The subvolcanic intrusions of latite, quartz latite, and rhyodacite are the products of differentiation (Fig. 24). Evidence from field relationships and petrologic data indicate that the differentiation did not occur with a continuous and predictable increase in alkali feldspar

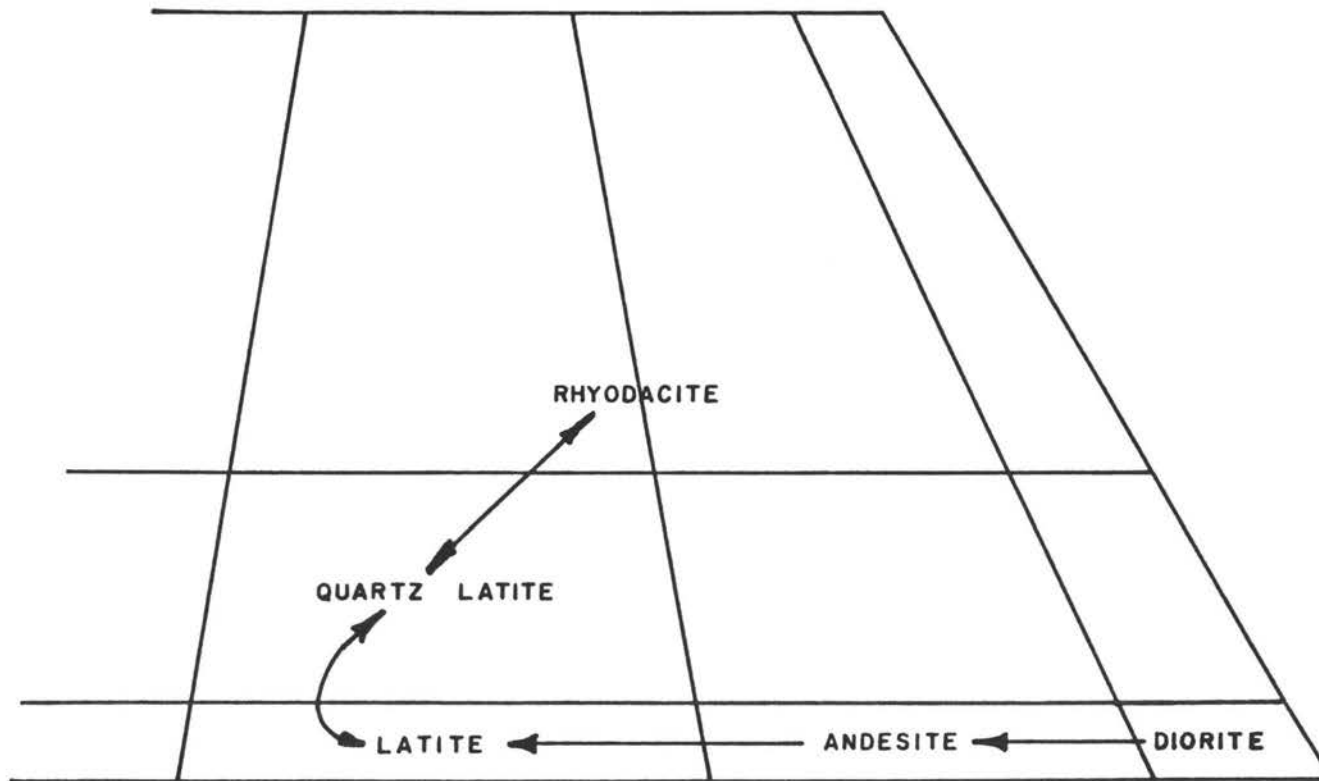


Figure 24. Diagram depicting the evolution of the intrusive rocks of the Alice E. vicinity. Data from Figure 8 of this study. Diagram adapted from Streckeisen (1979).

and quartz content, but that fluctuations between latite and rhyodacite compositions occurred (Fig. 24). Thus latite, quartz latite, and rhyodacite composition intrusions were formed at various times during the Eocene. Documented ages for many of these intrusives are not available, and local field relationships were used to determine the relative ages of the intrusions.

Chemical data for the rocks also show the evolution of the igneous complex (Fig. 25). Potash and silica contents increase as a result of differentiation.

The K_2O content at a SiO_2 content of 57.5 percent is 1.9 percent (Fig. 25). The rocks of the Cooke City intrusion are of the calc-alkalic suite according to the classification set forth by Westra and Keith (1981).

Other data (Eyrich, 1969) showed that potassium metasomatism was important in the latest stages of magmatic and ensuing hydrothermal activity that occurred in the area.

Trace element data for Absaroka volcanic rocks have been used to determine the origin of the volcanic rocks (Peterman and others, 1970). Their study utilized $^{87}Sr/^{86}Sr$ and $^{206}Pb/^{204}Pb$ isotopic ratios. The results suggest that the rocks were derived from the lower crust or upper mantle. It is evident that a preferential loss of uranium relative to lead occurred approximately 2,800 m.y. ago (Peterman and others, 1970). They relate small variations in isotopic ratios to small inhomogeneities in isotopic ratios in the source rocks.

A recent review of gold deposits in Montana (Cope, 1981) showed that the deposits are associated with both calc-alkalic and alkalic intrusive-volcanic complexes.

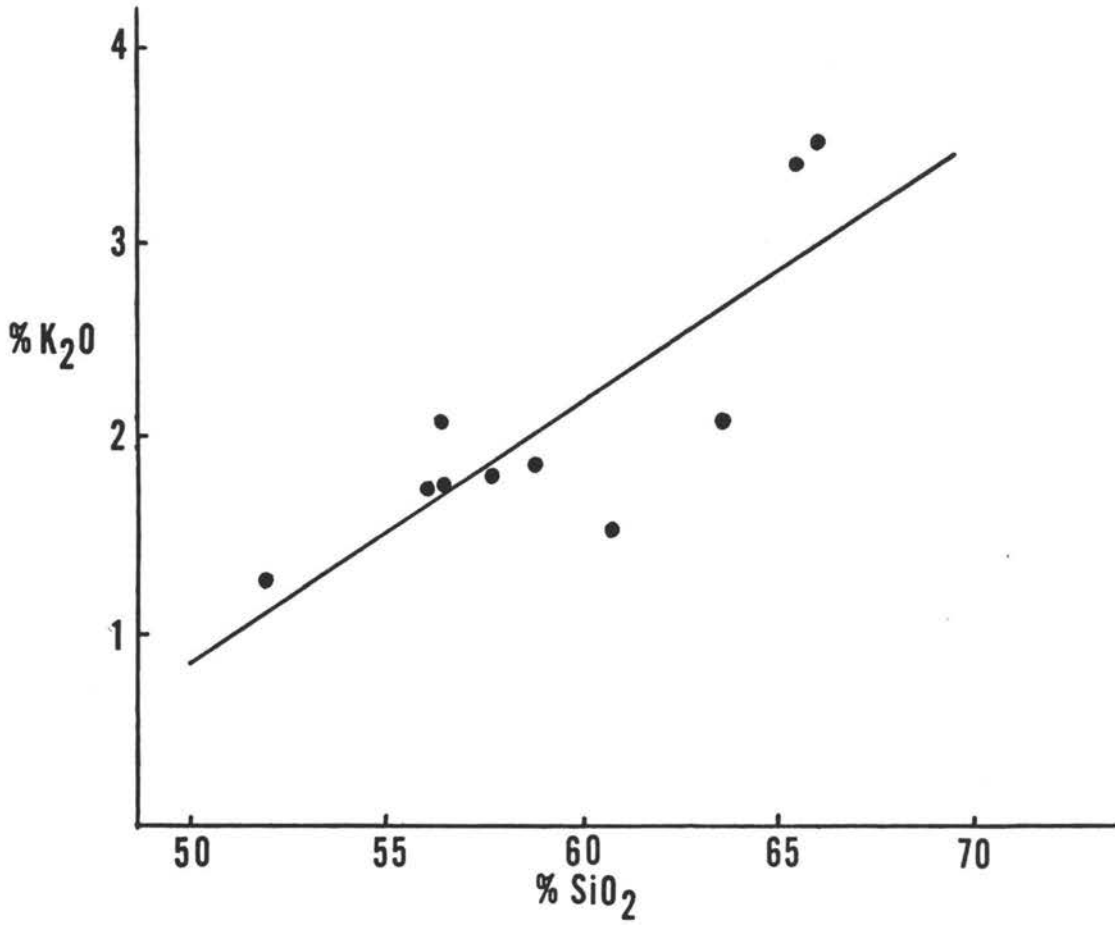


Figure 25. Harker variation diagram for K₂O-SiO₂. Data from Prostka (personal comm., 1982).

The style of gold deposits which occur in calc-alkalic complexes differ significantly from those gold deposits associated with alkalic complexes. The variation in pluton composition appears to be reflected in the ore deposits which in some cases can be shown to have formed long after the intrusion of the igneous body.

The major differences between the calc-alkalic and alkalic complexes are related to chemical composition involving primarily the SiO_2 , K_2O , CaO and Na_2O contents. Calc-alkalic deposits such as Cooke City are related to SiO_2 and K_2O rich late stage quartz-latitude porphyry intrusions. Alkalic type deposits (Zortman-Landusky, Little Rocky Mountains, Montana) are related to a syenite porphyry complex which is extremely potassic in nature but relatively silica poor.

The parent magma composition is largely responsible for the different types of hydrothermal alteration which accompany the two styles of deposits. The greater volatile content of a silica-rich late-stage calc-alkalic porphyry ("wet porphyry") will generate an extensive phyllic alteration (quartz-sericite-pyrite) outside a rather restricted potassic alteration zone. Stockworks and large breccia pipes are often associated with these complexes (i.e., Cooke City intrusive complex). Alkalic intrusions are silica deficient and also contain less volatiles ("dry porphyry") at the late stages of magmatic activity. The result is that phyllic alteration is rare with potassic alteration being common. Minor silica with sulfides and gold is deposited in joints and fractures in the pluton and as vein and replacements in rocks in contact with the pluton. Linear breccia bodies appear to be most important and large breccia pipes are less common.

In general, calc-alkalic porphyry gold occurrences exhibit a typical porphyry type alteration-mineralization zonation with a restricted potassic-ore zone and a large phyllic alteration halo. Alkalic porphyry gold deposits contain dominantly potassic alteration which accompanies the gold mineralization. The differences in alteration and mineralization can be linked to the composition of the late magmatic phases of the igneous complex.

The gold deposits of the New World District exhibit all of the characteristics common to calc-alkalic porphyries.

STRUCTURE

Bedrock structures are not well exposed in the vicinity of the Alice E. mine. The presence and location of many of the structures are inferred from evidence obtained at prospect pits in the area. Aerial photos were studied to aid in the mapping of some structures.

Faults

Two high angle faults appear as prominent features on aerial photos of the area. The faults intersect in Miller Creek (Plate 2) with an older N50°W trending fault offset by a younger fault trending N55°E. The older fault parallels the system of fractures of the Cooke City structural zone. The younger fault is probably related to jointing present in the Precambrian basement rocks. Both represent readjustment of fractures that formed at some time in the history of the Beartooth block, previous to the Laramide Orogeny. The structures are probably of Precambrian origin with recent (Laramide) displacement of not more than 200 feet as indicated by Elliott's (1979) map.

Veins and Dikes

Mineral veins and dikes are observed occupying a number of structures that formed during the intrusion of the igneous bodies within the study area.

Quartz-sulfide veins of open space origin cut igneous and sedimentary units in the eastern part of the study area. The veins occur

in and adjacent to the breccia pipe in the fractures that postdate brecciation and coincide with intrusion of the biotite latite porphyry stock. The veins are aligned in a crudely radiating pattern in rocks surrounding the southeast part of the stock (Plate 2). Mineralizing fluids ascended through the open spaces created by brecciation and fracturing of the country rock in the area.

Dikes occur in the breccia pipe and the area peripheral to the breccia pipe. The dikes are linear, or in radial or arcuate patterns (Plate 2). The age of the structures coincide with the breccia event. The patterns are similar to those observed for volcanic pipes of the San Juan volcanic field (Burbank, 1939).

Sheet and Stockwork Fracturing

Parallel to subparallel sheet-like fractures are observed in Flathead Sandstone at the Alice E. mine. Oxidized quartz-sulfide veinlets occupy these sheet fractures. Sheet fracturing is present at most breccia pipes described in the literature. The fracturing occurred as a late event in the breccia pipe genesis.

Stockwork fractures with quartz fillings are observed in granite and diorite in Miller Creek. Vein and disseminated sulfide mineralization are related to these fractures. The stockwork consists of quartz veins in densities ranging from low to moderate (1 to 3 veins per square foot). Stockwork fracturing is an integral part of porphyry molybdenum and copper deposits. Most workers relate the fracturing to late magmatic-hydrothermal processes (Burnham and Ohmoto, 1980) and probable boiling of hydrothermal fluids (Cunningham, 1978). The

fracturing and subsequent vein filling localizes much of the ore in deposits of the porphyry type.

HYDROTHERMAL ALTERATION

Extensive hydrothermal alteration accompanied sulfide mineralization in the New World Mining District. At the Alice E. three alteration types are recognized. These include a regional propylitization which has been overprinted by localized zones of phyllic alteration and hydrous skarn type alteration. Potassium silicate minerals are observed as open-space breccia fillings with skarn minerals.

Clay minerals are abundant locally and are of supergene origin in areas of sulfide oxidation.

Propylitic Alteration

Propylitic alteration (Creasy, 1966; Rose and Burt, 1979) is widespread in the rocks surrounding the Alice E. breccia pipe (Plate 2). Chlorite, epidote, calcite, and magnetite are common secondary minerals in zones of propylitic alteration in the area. Sericite and montmorillonite are usually present in small quantities.

Propylitic alteration is reported at most porphyry Cu-Au deposits. Gold-bearing porphyry deposits in Canada consistently have propylitic alteration peripheral to a centralized potassium silicate alteration (Barr et al., 1976).

Chemical data are not available but crude estimates of chemical changes due to alteration may be inferred from the propylitic mineral assemblage. Rose and Burt (1979) state that little cation metasomatism occurs, but that H_2O , CO_2 , and S may be added. Hemley and Jones

(1964) show that the gain of Na^+ , Ca^{2+} , Mg^{2+} , and SiO_2 is likely to occur, while the activity of H^+ will decrease and the activity of K^+ will remain the same.

Mineral stabilities for the propylitic assemblage indicate that the altering fluids were $<400^\circ\text{C}$ and neutral to alkaline (Stringham, 1952).

Propylitic alteration is most common in the biotite latite porphyry stock, and the sills of diorite, trachyandesite porphyry, and rhyodacite porphyry. Propylitic alteration is observed in the more weakly mineralized parts of the breccia pipe.

The intensity of alteration is variable and related to factors such as proximity to mineralizing plutons and the permeability (fracture density) of the rock.

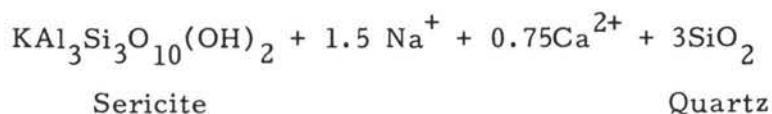
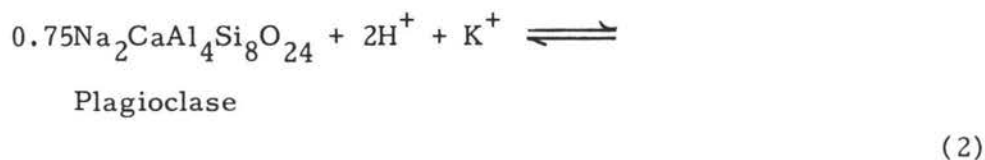
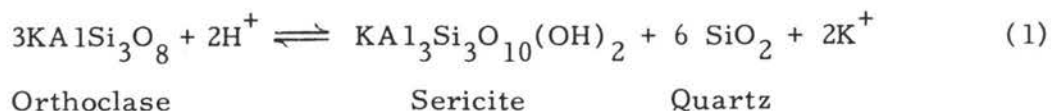
Phyllic Alteration

The term phyllic alteration (Lowell and Guilbert, 1970) is used where the secondary mineral assemblage is quartz, sericite and pyrite. In the Alice E. vicinity phyllic alteration occurs in the breccia pipe and surrounding rocks. The Precambrian granite, the biotite latite porphyry stock, the diorite sill and the sandy fragments of the breccia pipe are all noted to exhibit phyllic alteration.

Plagioclase and potassium feldspar in igneous rock types are converted to sericite and carbonate. Silica is often added as flooding and as veins and veinlets often with pyrite.

Tourmaline (?) was observed as a vein mineral in an example of phyllic altered sandstone at the Alice E.

The alteration of feldspars to sericite may occur by the reactions established by Hemley and Jones (1964):



The reactions show that potash and silica are added and sodium and calcium are leached. Calcite may form in the presence of CO_2 .

The areas of phyllic alteration are indicated on the alteration map (Plate 2). Examples of strongly altered dike rocks (Figs. 26 and 27) clearly show the mineralogic changes that occur in rocks altered to the phyllic assemblage.

As in other alteration types, the intensity of alteration is often related to the fracture density present in the rock.

Hydrous Skarn Alteration

Endoskarn and exoskarn calc-silicate alteration (Einaudi, 1982) is present in the Alice E. breccia pipe. These alteration types are particularly conspicuous in and adjacent to the crescent-shaped quartz amphibole latite porphyry located at the northwest corner of the breccia pipe.

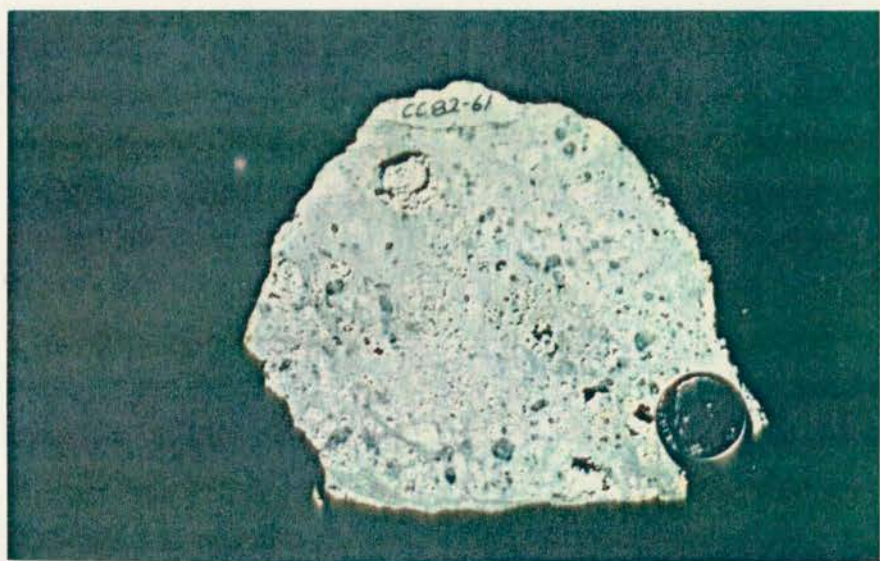
Garnet (andradite) is present in the porphyry at the location mentioned above. The garnets were observed in a narrow zone at the contact between porphyry and breccia. Einaudi (1982) cites this as

The first part of the paper is devoted to the study of the
 asymptotic behavior of the solutions of the system
 (1.1) as $\epsilon \rightarrow 0$. In the second part, we study the
 asymptotic behavior of the solutions of the system
 (1.2) as $\epsilon \rightarrow 0$. In the third part, we study the
 asymptotic behavior of the solutions of the system
 (1.3) as $\epsilon \rightarrow 0$. In the fourth part, we study the
 asymptotic behavior of the solutions of the system
 (1.4) as $\epsilon \rightarrow 0$. In the fifth part, we study the
 asymptotic behavior of the solutions of the system
 (1.5) as $\epsilon \rightarrow 0$. In the sixth part, we study the
 asymptotic behavior of the solutions of the system
 (1.6) as $\epsilon \rightarrow 0$. In the seventh part, we study the
 asymptotic behavior of the solutions of the system
 (1.7) as $\epsilon \rightarrow 0$. In the eighth part, we study the
 asymptotic behavior of the solutions of the system
 (1.8) as $\epsilon \rightarrow 0$. In the ninth part, we study the
 asymptotic behavior of the solutions of the system
 (1.9) as $\epsilon \rightarrow 0$. In the tenth part, we study the
 asymptotic behavior of the solutions of the system
 (1.10) as $\epsilon \rightarrow 0$.

The first part of the paper is devoted to the study of the
 asymptotic behavior of the solutions of the system
 (1.1) as $\epsilon \rightarrow 0$. In the second part, we study the
 asymptotic behavior of the solutions of the system
 (1.2) as $\epsilon \rightarrow 0$. In the third part, we study the
 asymptotic behavior of the solutions of the system
 (1.3) as $\epsilon \rightarrow 0$. In the fourth part, we study the
 asymptotic behavior of the solutions of the system
 (1.4) as $\epsilon \rightarrow 0$. In the fifth part, we study the
 asymptotic behavior of the solutions of the system
 (1.5) as $\epsilon \rightarrow 0$. In the sixth part, we study the
 asymptotic behavior of the solutions of the system
 (1.6) as $\epsilon \rightarrow 0$. In the seventh part, we study the
 asymptotic behavior of the solutions of the system
 (1.7) as $\epsilon \rightarrow 0$. In the eighth part, we study the
 asymptotic behavior of the solutions of the system
 (1.8) as $\epsilon \rightarrow 0$. In the ninth part, we study the
 asymptotic behavior of the solutions of the system
 (1.9) as $\epsilon \rightarrow 0$. In the tenth part, we study the
 asymptotic behavior of the solutions of the system
 (1.10) as $\epsilon \rightarrow 0$.

Figure 26. Cut specimen of phyllic altered dike rock. Sample is pervasively altered to quartz and sericite. Rounded quartz phenocrysts are stable. Feldspars and mafic minerals are completely altered. Note quartz veining.

Figure 27. Cut specimen of altered quartz amphibole latite porphyry. Sample is phyllic altered with pyrite. Note silica flooding and intense sericitization.



evidence for fluid flow upward along the contact and into the pluton. This is typical of endoskarn alteration observed at many porphyry-skarn deposits.

Exoskarn alteration at the Alice E. breccia pipe is characterized by the assemblage actinolite, epidote, chlorite and magnetite. This occurs as massive replacements of carbonate breccia fragments. The contact between the quartz amphibole latite porphyry and the breccia (Fig. 28) shows the endo- exo-skarn relationships discussed here. Xenoliths of altered wall rock are present in the porphyry. Thin sections (Fig. 29) show the mineralogy of the alteration to be the same as that observed in the wall rocks.

At one location near the Alice E. mine the breccia is cemented by quartz and adularia which are replaced by calcite and actinolite (Figs. 30 and 31). Quartz-epidote veinlets in the breccia are the same age as the open space filling, and the veinlets often emanate from the breccia matrix and cut breccia fragments. This alteration post-dates the development of the breccia.

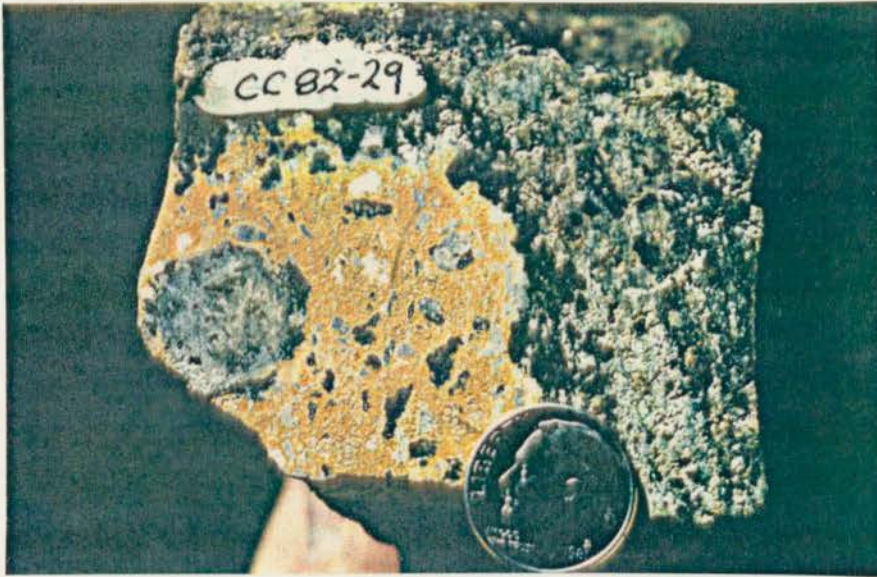
The actinolite in the quartz amphibole latite porphyry may be partly of hydrothermal origin. Actinolite has been reported in the Rialto stock, New Mexico (Thompson, 1968) and in quartz monzonite porphyry at Bingham Canyon, Utah (Lanier, 1975).

Skarn alteration at the Alice E. breccia pipe is similar to the late hydrous alteration observed by Atkinson (1975) at Carr Fork, Utah, although no orbicular textures are noted at the Alice E.

The Capote breccia pipe at Cananea, Mexico has quartz-actinolite alteration in limestone (Meinhert, 1982) which replaces earlier garnet-pyroxene skarn and marble. Extensive garnet-pyroxene skarn is not

Figure 28. Photograph showing contact between quartz amphibole latite porphyry and breccia pipe material. Sample stained for potassium feldspar. Note epidote-actinolite alteration rind adjacent to porphyry, and xenolith in porphyry showing similar alteration. Note high potassium feldspar content of porphyry.

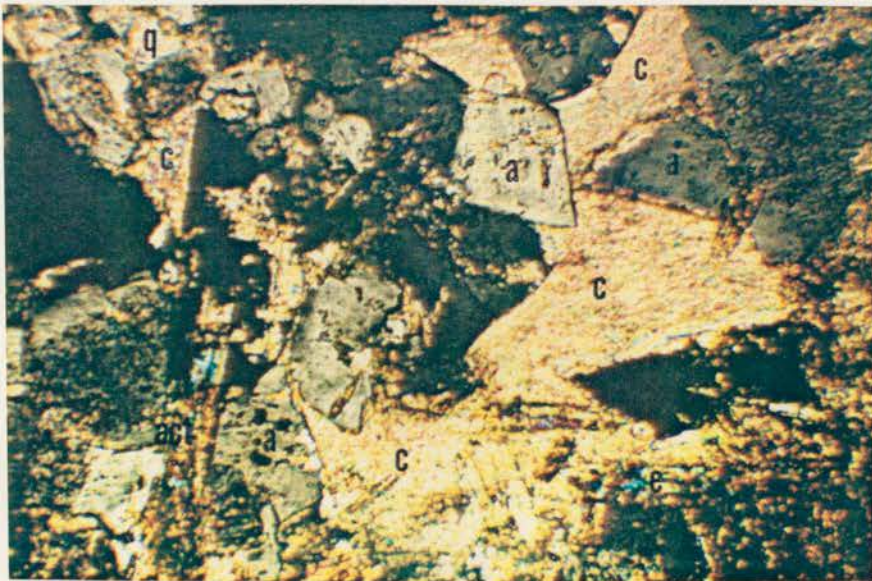
Figure 29. Photomicrograph of sample CC-82-29 (crossed nicols). Epidote-actinolite alteration of xenolith in porphyry shown in Figure 28. Epidote (e); actinolite (act).



0.1mm

Figure 30. Cut specimen of breccia pipe material (Tbx). Breccia fragments are Flathead Sandstone. Matrix is post-breccia epidote, actinolite, quartz, adularia and pyrite.

Figure 31. Photomicrograph of sample CC-82-53 (crossed nicols). Open space deposition of actinolite (act), epidote (e), adularia (a), quartz (q) and calcite (c) in breccia voids.



0.1mm

present at the Alice E. breccia pipe. The lack of garnet-pyroxene skarn is either the result of complete masking by later hydrous skarn or the lack of any original early garnet-pyroxene skarn alteration.

Explanation of the skarn assemblage at the Alice E. is possible by reconstructing the pressure and temperature conditions at the time of alteration. The field relationships indicate that a subvolcanic environment prevailed in which pressures would not be high. The combination of high temperatures and relatively low pressures may explain the assemblage.

SUPERGENE ALTERATION

Supergene alteration superimposed on hypogene hydrothermal alteration is common at many porphyry copper deposits (Rose, 1970). This alteration occurs due to the formation of acids as pyrite is oxidized. Supergene enrichment of sulfides may occur if sufficient pyrite is present in the protore.

Surface samples collected from the Alice E. area show that supergene alteration has occurred to a limited degree in a few sulfide-rich zones.

Kaolinite and Fe-oxides (limonite) are common products of this alteration. Secondary copper sulfides (digenite, covellite) are present at one locality just outside the breccia pipe.

Supergene alteration is most prevalent in areas of intense phyllic alteration where significant pyrite is often present. Glaciation has probably removed much supergene altered material from the area.

MINERALIZATION

Mineralization consisting of three hypogene events occurred in and around the Alice E. breccia pipe. The mineralization consists of high temperature quartz sulfide veins, veinlets and stockworks associated with zones of phyllic alteration, and sulfide replacement of carbonate breccia fragments and wall rocks which is intimately related to the skarn type alteration. These two types of alteration-mineralization are related to wall rock composition, with the vein type mineralization occurring in the Precambrian basement rocks, the Tertiary intrusive rocks, and the Flathead Sandstone. The skarn-replacement mineralization-alteration occurs in carbonate host rocks. The third type of mineralization is a late open space deposition of calcite with base metal sulfides that occurs in the breccia and veins in the vicinity.

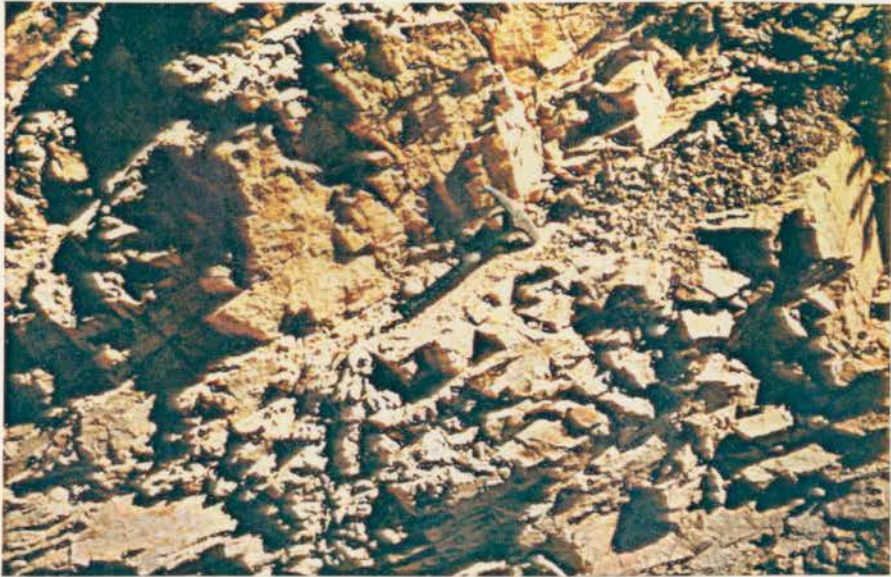
Vein Mineralization

High temperature quartz-sulfide veins and veinlets occur at a number of localities within the study area (Plate 2). The veins are observed as parallel sheet fracture fillings at the Alice E. mine and as stockworks in Miller Creek.

Sheet fracture veins at the Alice E. mine occur in a disrupted block of Flathead Sandstone (Figs. 32 and 33). The veins are oxidized quartz-sulfide veins containing significant gold and silver. Much of the production from the Alice E. mine came from this zone.

Figure 32. Photograph of sheet fractured zone at the Alice E. mine. Zone is oxidized with silica and limonite remaining. This zone assayed 10.58 ppm Au.

Figure 33. Closeup of sheet fractures in sandstone at the location in Figure 33. Note parallel nature of quartz veining.



Quartz-sulfide veins are observed cutting the trachyandesite porphyry sill in the eastern part of the study area. These veins are usually a few to tens of centimeters in width and can be traced for short distances along strike in prospects. The veins are arranged in a crude radial pattern about the south end of the latite porphyry stock.

The stockwork veining in Miller Creek is weakly to moderately developed (1 to 3 veinlets per square foot). Sulfide minerals are vein-controlled and disseminated throughout the stockwork zone.

Sulfide minerals present in areas of vein mineralization consist of pyrite, chalcopyrite, and bornite. Digenite and covellite were observed in one oxidized pyrite-chalcopyrite vein specimen. Quartz and calcite are common gangue minerals of vein type mineralization.

Skarn-Replacement Mineralization

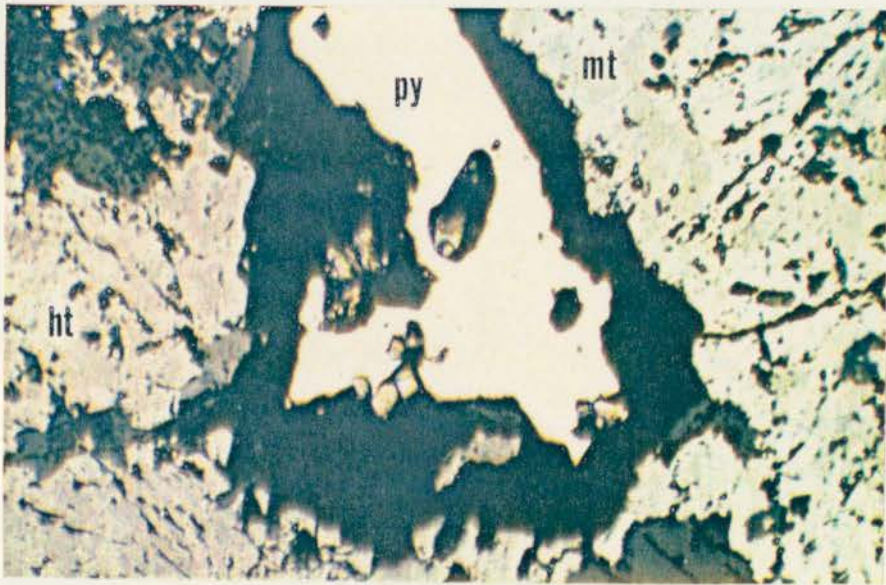
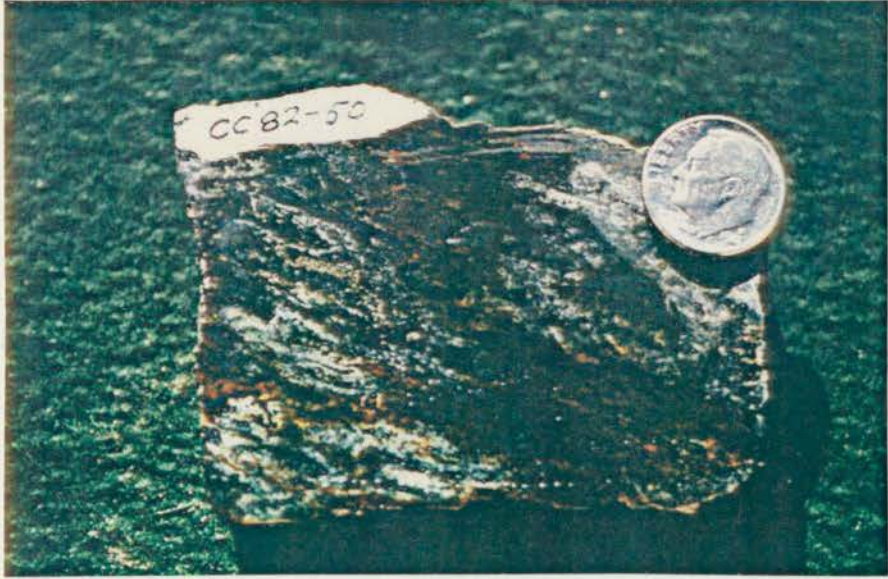
Fragments of breccia and wall rock that contained significant lime have undergone replacement by oxide and sulfide minerals.

Massive magnetite with later sulfides have replaced breccia in the western part of the pipe. The massive bodies are replaced fragments and blocks of Meagher Limestone and possibly Pilgrim Limestone. Replacement mineralization occurs in Wolsey Shale at the northeast corner of the breccia pipe. Oxide and sulfide minerals are present as irregular replacements of the sediments (Figs. 34 and 35). Replacement minerals consist of magnetite, pyrite, chalcopyrite, and sphalerite.

Open space mineralization consisting of sulfide and skarn assemblage minerals occurring in the breccia are related to the replacement

Figure 34. Cut specimen of Wolsey Shale (Cw) replaced by magnetite and pyrite. Hematite and oxides rich in lead? (white color) are also present.

Figure 35. Polished section photomicrograph of sample CC-82-50 (plane reflected light). Magnetite (mt) is replaced by hematite (ht) and pyrite (py).



0.1mm

mineralization. This is a partial replacement of comminuted breccia matrix with late open space filling by skarn minerals.

Gold mineralization is present in skarn-replacement zones.

Paragenesis

The paragenetic sequence for mineralization at the Alice E. (Fig. 36) was determined from thin sections and polished specimens of mineralized samples.

Stage I

Stage I mineralization is characterized by massive replacement of carbonate rocks. Quartz and magnetite (Fig. 35) are the main products of this replacement. The early oxide mineralization is followed by stage II mineralization consisting of vein sulfides.

Stage II

Stage II mineralization consists of Cu and Fe sulfide minerals. Pyrite, chalcopyrite, and bornite were deposited at this time.

Stage II vein mineralization is made up of early massive pyrite that is cut by chalcopyrite-bornite veinlets (Fig. 37). This is the main sulfide mineralization event.

Gold was not visible in the polished sections that were examined, however anomalous amounts of gold were detected in the geochemical analyses of the sulfide specimens. This evidence leads me to believe that the gold was introduced in the sulfide stage and probably accompanied the pyrite-chalcopyrite-bornite mineralization. This is evident in the geochemistry which shows a strong Cu-Au relationship.

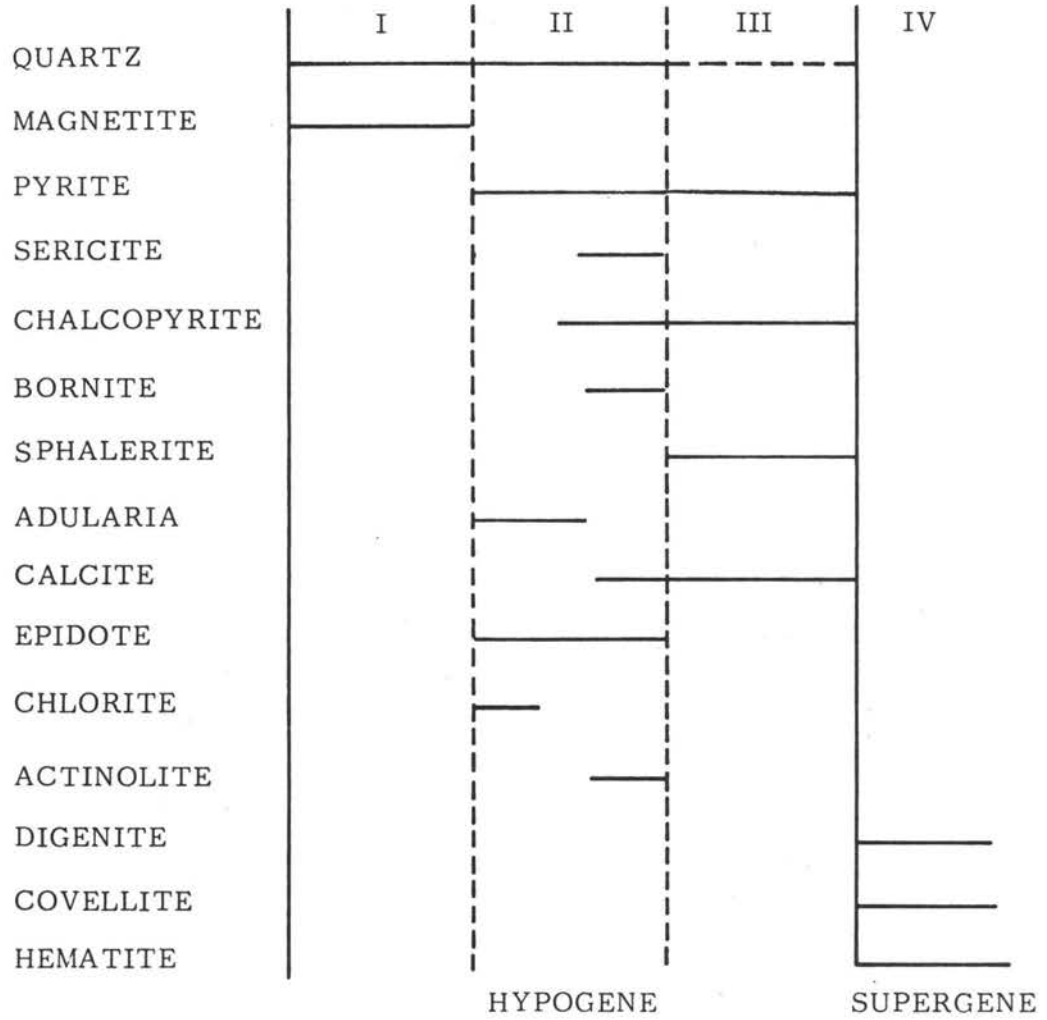
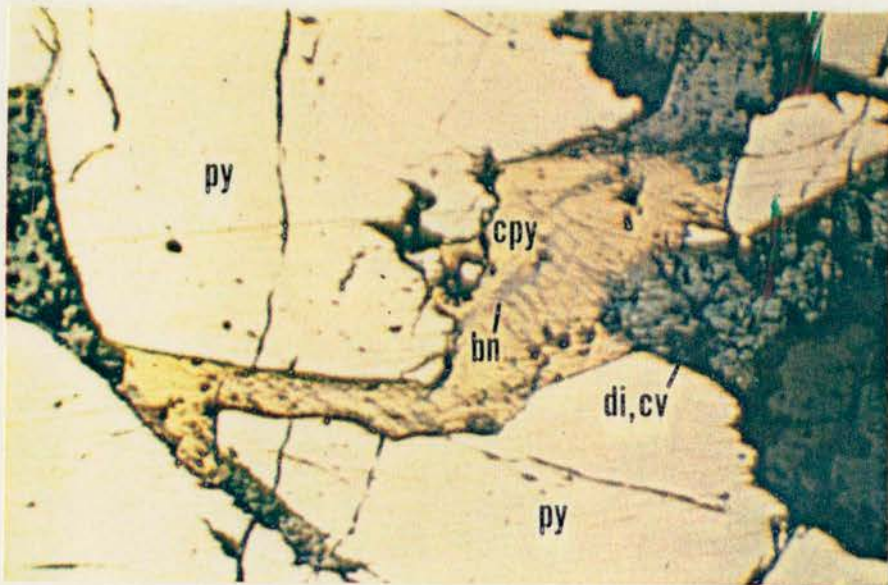


Figure 36. Paragenetic diagram for mineralization at the Alice E. mine and vicinity.



0.1mm

Figure 37. Polished section photomicrograph of sample CC-82-52 (plane reflected light). Quartz vein with early pyrite (py) cut by veinlets of chalcopyrite (cpy). Bornite (bn) slightly postdates chalcopyrite. Note secondary copper sulfides digenite (di) and covellite (cv).

Stage III

The last hypogene mineralization is a replacement and open space mineralization event with calcite, pyrite, chalcopyrite (Fig. 38) and sphalerite as the main minerals. Strong exsolution chalcopyrite occurs in sphalerite (Fig. 39). This type of mineralization occurs as late breccia cavity filling and in replacement bodies. Carbonate minerals are observed with sulfides as coprecipitates in this stage of mineralization.

Stage IV

Supergene oxidation of pyrite and other sulfides is evident in many samples from the Alice E. area. Chalcopyrite-bornite veins are replaced by digenite (Fig. 40).

Geochemical data suggests that supergene processes have enriched gold and silver at the Alice E. mine, while copper was leached from these rocks.

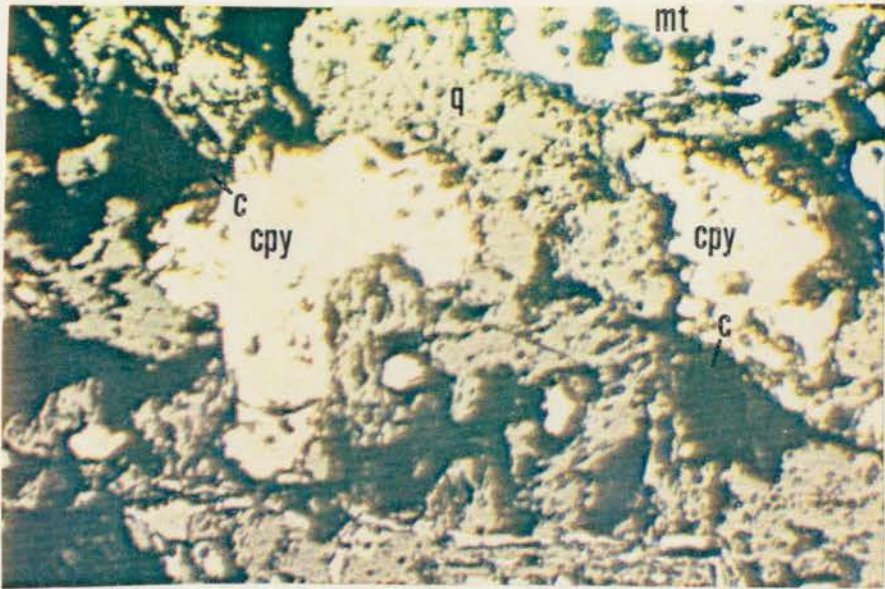
Hematite replacing pyrite (Fig. 41) is common in zones of oxidation, as are other limonites.

The first step in the development of a new product is the identification of a market need. This is often done through market research, which can be conducted in a number of ways. One common method is to conduct focus groups, where a small group of people are brought together to discuss their needs and preferences. Another method is to conduct surveys, which can be distributed to a large number of people. Once a market need has been identified, the next step is to develop a product concept. This is often done through brainstorming sessions with a team of designers and engineers. The product concept should be based on the market need and should be designed to meet the needs of the target market.

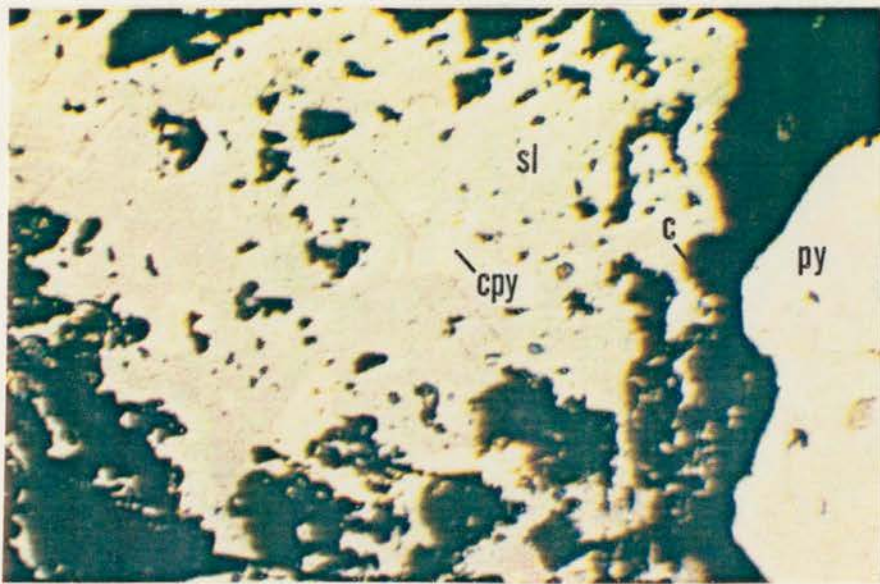
The second step in the development of a new product is the design and development of the product. This is often done through a process of iterative design, where the product is designed and then tested, and the design is refined based on the results of the testing. This process can be repeated as many times as necessary to ensure that the product is designed to meet the needs of the target market. Once the product has been designed and developed, the next step is to conduct a pilot test. This is often done to ensure that the product is manufacturable and that it can be sold at a profit.

Figure 38. Polished section photomicrograph of sample CC-82-33 (plane reflected light). Massive magnetite (mt) with quartz (q) replacement of carbonate rock. Chalcopyrite (cpy) with carbonate (c) is later replacement sulfide stage.

Figure 39. Polished section photomicrograph of sample CC-82-35 (plane reflected light). Open space deposition of pyrite (py) and sphalerite (sl) with strong exsolution chalcopyrite (cpy). Gangue is calcite (c).



0.1mm



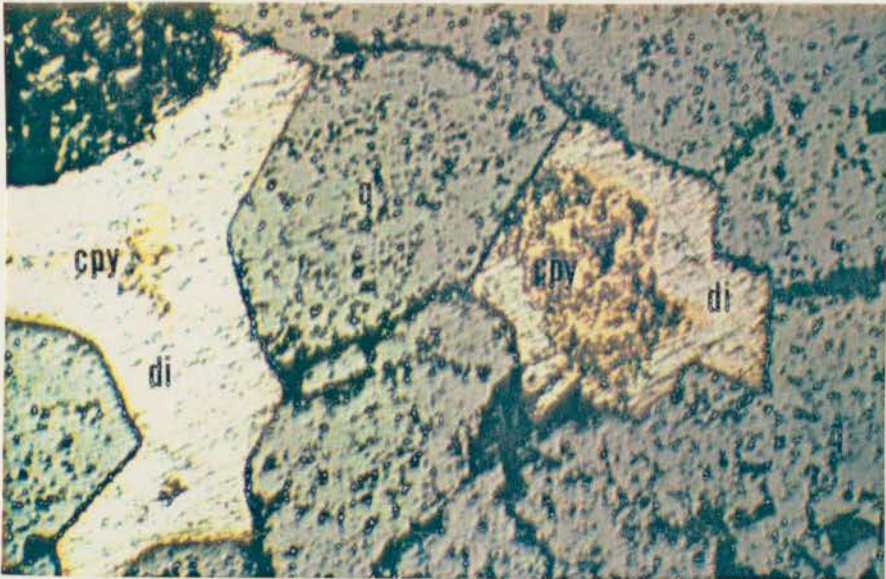
0.1mm

The first part of the paper is devoted to the study of the
 asymptotic behavior of the solutions of the system
 (1.1) as $t \rightarrow \infty$. It is shown that the solutions
 tend to zero as $t \rightarrow \infty$ if and only if
 the matrix A is stable.

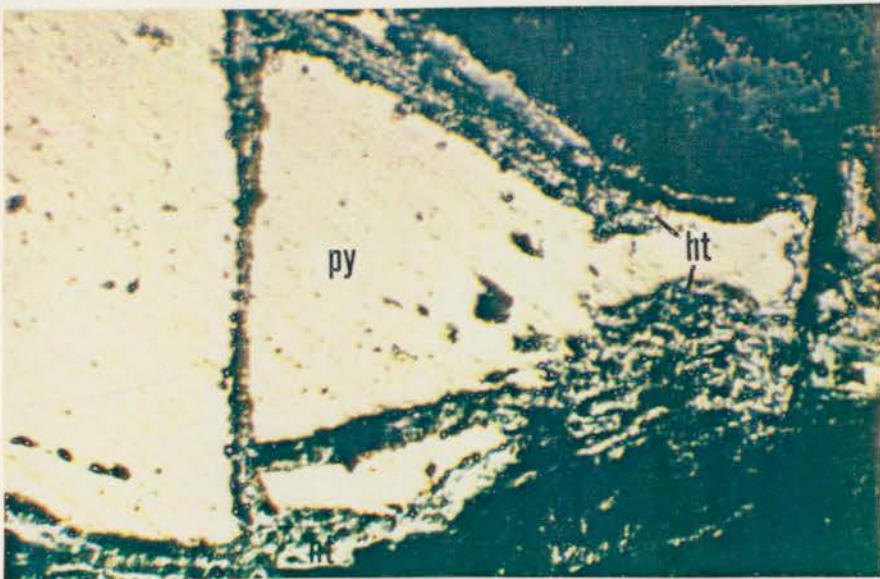
In the second part of the paper the problem of the
 asymptotic stability of the solutions of the system
 (1.1) is considered. It is shown that the system
 (1.1) is asymptotically stable if and only if
 the matrix A is stable and the matrix
 B is nonsingular.

Figure 40. Polished section photomicrograph of sample CC-82-52 (plane reflected light). Quartz (q) with chalcopyrite (cpy) and digenite (di) from weakly oxidized pyrite-chalcopyrite-bornite quartz vein.

Figure 41. Polished section photomicrograph of sample CC-82-30 (plane reflected light). Pyrite (py) replaced by supergene hematite (ht) in moderately oxidized replacement ore.



0.1mm



0.1mm

FLUID INCLUSIONS

Thin sections cut from samples collected in 1981 contain abundant fluid inclusions. Fluid inclusions were observed in igneous quartz and quartz veins from samples collected at the Alice E., and plans were made to study the inclusions as part of the thesis. The specimens collected in 1982 were carefully chosen to represent the gold mineralization present in the Alice E. area. Gold was detected in all of the samples from which polished plates were prepared.

The fluid inclusion study was limited to heating studies due to the fact that many of the inclusions were too small to freeze or they contained halite daughter crystals which enable salinity estimates to be made during heating.

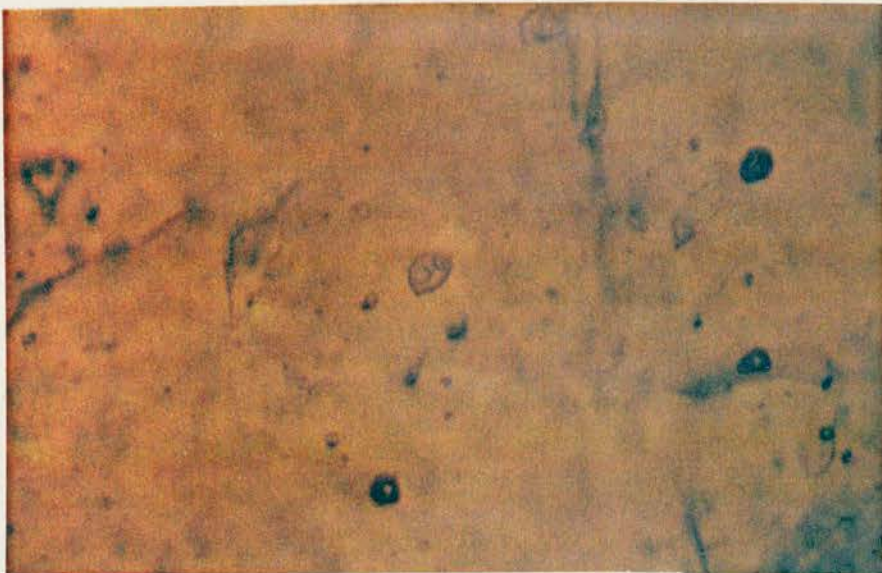
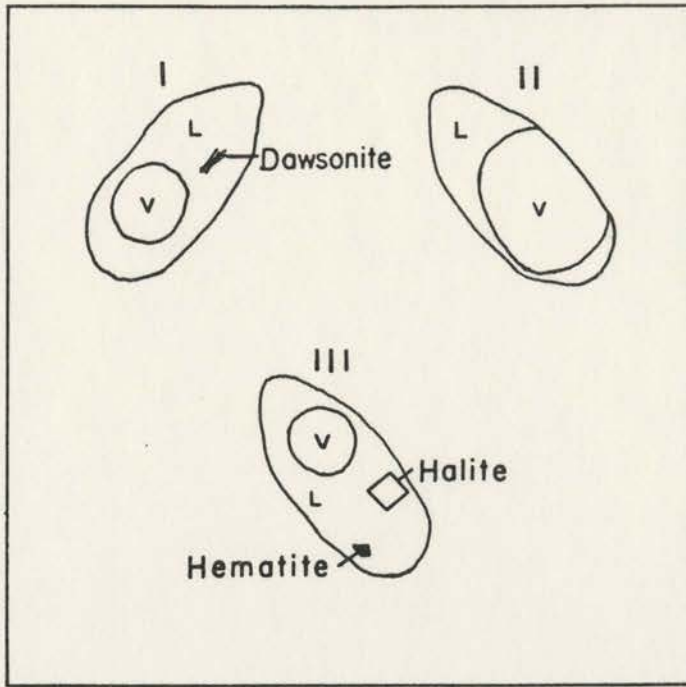
Types of Inclusions

Numerous schemes have been used to classify fluid inclusions. The classifications used by Nash (1976) has four types of inclusions which are based on phase relationships which are observable under an ordinary petrographic microscope. The four types are: 1) two phase liquid-dominated with vapor; 2) gas rich; 3) halite-bearing; and 4) CO₂ rich.

The first three types are present in Alice E. samples but CO₂-rich inclusions were not observed. The phase relationships of inclusions observed are presented in Figures 42 and 43.

Figure 42. Sketches of fluid inclusion types observed in Alice E. vein and open space breccia filling quartz (Adapted from Nash, 1976).

Figure 43. Polished plate photomicrograph of sample CC-82-53 (plane light). Halite-bearing primary (Type III) fluid inclusion in open space breccia quartz with pyrite-gold mineralization. The halite-bearing inclusion in the center of the photo is approximately 10 microns in length.



Two Phase Liquid-Dominated Inclusions (Type I)

The most common inclusions in Alice E. vein quartz contain two phases and occasional birefringent (dawsonite?) and opaque daughter minerals. Estimations of salinity are crude but based on the fact that no halite daughter crystals were observed, these inclusions contain less than 23 wt. % NaCl.

The inclusions are liquid dominated with vapor content at room temperature (18°C) averaging 20 volume percent.

Gas Rich Inclusions (Type II)

Gas rich inclusions occur in one sample from the Alice E. vicinity. The sample is from the stockwork zone exposed in Miller Creek. These inclusions show a large variation in liquid to vapor ratios and are often gas dominated. In other aspects these inclusions are similar to Type I inclusions.

Halite-Bearing Inclusions (Type III)

Halite daughter crystals were observed in inclusions in igneous quartz phenocrysts and quartz veins. They are the second most abundant type of inclusions in the Alice E. area.

Opaque to reddish (hematite?) daughter minerals are common in Type III inclusions. Anhydrite(?) was observed in a few inclusions during the study.

Type III fluid inclusions are liquid dominated with vapor contents of 5 to 20 volume percent observed in vein specimens. Type III

inclusions occur throughout the area investigated and may occur with Type I and or Type II inclusions in the same sample.

Homogenization Temperatures

Heating studies were conducted using a calibrated Roman Science heating stage.

The vein samples contain abundant inclusions. Primary and pseudo-secondary inclusions were selected for homogenization temperature determination. Secondary inclusions formed in healed fractures were avoided due to their uncertain origin.

The heating studies show that the homogenization temperatures for inclusions in ore stage quartz range from 320°C to temperatures which exceeded the limits of the heating apparatus (530°C) (Table 6).

Homogenization temperatures for inclusions in discrete samples often yielded highly variable temperatures as is demonstrated in Table 6 and Appendix Table 11.

The data are presented on the mineralization map (Plate 2) to show the spatial relationships of the veins that were studied.

The highest temperatures were observed in a sample from the stockwork zone. Breccia pipe samples and vein samples from the eastern part of the study area all contain inclusions that homogenized at much lower temperatures than those from the stockwork zone. The highest temperatures occur in the lowermost exposed mineralized zone suggesting that a vertical temperature zonation existed in the hydrothermal system depositing the quartz veins.

Table 6. Fluid inclusion data obtained from heating stage study. Filling (homogenization) temperatures are for quartz from vein and breccia samples located on Plates 1 and 2.

Sample	Inclusion Types	Filling Temp. Range (°C)	Mean Filling Temp. (°C)	Replicate Analyses (°C)	Inclusions Analyzed
CC-82-1	I, III	327 to 426	380	± 3	21
CC-82-52	I	342 to 421	370	± 3	5
CC-82-53	I, III	352 to 470	398	± 3	10
CC-82-60	I, III	319 to 321	320	± 2	4
CC-82-63	II, III	447 to 530+	?	± 5	4

Gas-rich inclusions present in the stockwork zone are evidence that boiling accompanied mineralization in the zone now exposed in Miller Creek.

Lateral temperature zonation in quartz veins is exhibited in the veins throughout the east part of the thesis area. Temperatures decrease towards the margins of the breccia pipe and show a decrease in temperature away from the breccia in veins up to 1,000 feet from the pipe, where the coolest temperatures (320°C) were recorded (Plate 2).

Fluid inclusion homogenization temperatures are similar to those reported for porphyry deposits (Nash, 1976) and breccia pipe deposits (Sillitoe and Sawkins, 1971; Carlson and Sawkins, 1980). These data clearly establish the Alice E. mineralized zones as high temperature and "porphyry"-related.

Salinity

Salinities of halite-bearing (Type III) inclusions were determined by observing the dissolution of the halite cubes upon heating. The salinity of inclusions is generally greater than 30 wt. % NaCl and in some inclusions may approach 60 wt. % NaCl. The salinity data were obtained by plotting the dissolution temperatures on a standard curve (Fig. 44) for halite dissolution. The highest salinities were encountered in inclusions whose halite cubes did not dissolve at temperatures above 500°C.

The presence of vapor-rich inclusions (sample CC-82-63) is evidence that boiling occurred at a level that is now exposed in Miller Creek. Halite-bearing inclusions are abundant in samples collected

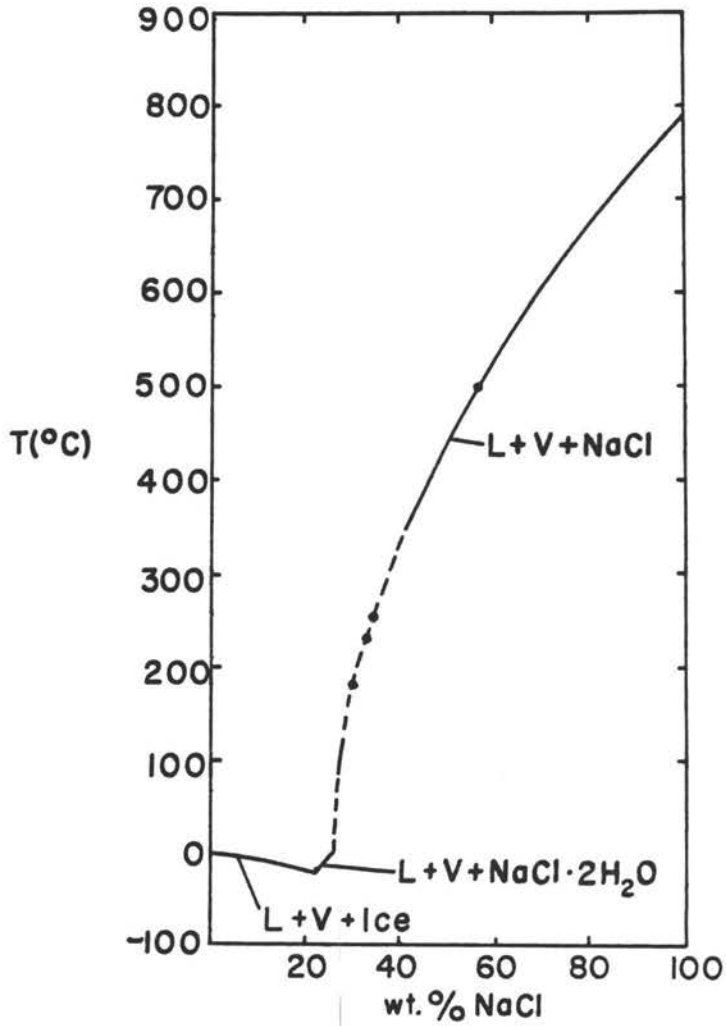


Figure 44. T-X projection in the system NaCl-H₂O. Note dissolution temperatures of halite in Alice E. Type III inclusions. Diagram from Erwood and others (1979).

from the stockwork in Miller Creek and in veins and breccia which are exposed at higher elevations in the study area. The high salinities observed may be the result of boiling concentrating NaCl by simple distillation. On the other hand, primary halite-bearing inclusions are abundant in igneous quartz phenocrysts suggesting that the late phase quartz rich porphyries were distinctly saline at the time of crystallization. It is probable that the late magmatic hydrothermal fluids were highly saline and through boiling, salinity was maintained even though much of the hydrothermal fluid may have been of meteoric origin.

The evidence of boiling and the presence of a highly saline ore fluid provide conditions that will allow the transport and deposition of gold, copper, and zinc from a high temperature ore fluid.

GEOCHEMISTRY

A total of 55 samples were collected for geochemical analysis during the 1981 and 1982 field seasons. The samples are all rock chip samples collected from pits, dumps and mineralized outcrops. Elements selected for analysis include Au, Ag, Cu, Mo, Pb, Zn and Te (Table 7, Appendix).

The small sample population prohibits detailed statistical analysis of the data, however certain geochemical trends can be inferred from the data. A brief discussion of the distribution of these elements in the study area will help in developing the model for ore deposition at the Alice E.

Gold

Gold was detected in 45 of 55 samples analyzed. Gold content in these samples ranged from the detection limit of 0.03 ppm to a high of 10.58 ppm.

The highest grade samples were collected from the sheet fractured zone of the Alice E. mine. Sampling and analyses indicate that gold content is dependent on the degree of silicification-veining in this zone.

Most gold-bearing samples from the Alice E. are oxidized to some extent. The oxidation of copper-gold pyritic ores would leave a residual of Fe-oxides and gold. This is the case for Alice E. oxide samples.

Other gold-bearing rocks in the area include mineralized breccia, quartz veins and stockworks, mineralized dikes, and rocks pervasively mineralized with disseminated sulfides.

Silver

Silver was found in detectable amounts in fewer rocks than gold in the study area. Anomalous amounts of silver occur in only a few specimens from the oxide zone of the Alice E. Silver is often easily enriched in the supergene environment and this clearly is the case at the Alice E.

It should be noted that most of the silver in the New World Mining District is found in replacement and vein deposits in carbonate rocks that surround the district. The deposits of the central portions of the district are gold dominated. The early work of Lovering (1929) documented the precious metal zoning.

Copper

Copper was found in amounts ranging from 10 ppm to 0.125 percent. Anomalous copper in the District samples is often associated with gold and sometimes with molybdenum. Copper and gold are found together throughout the central portions of the New World District.

Copper minerals present in the Alice E. ore assemblage are chalcopyrite (CuFeS_2), bornite (Cu_5FeS_4), digenite (Cu_{2-x}S), and covellite (CuS).

Molybdenum

Molybdenum was detected in most samples of the study. Values ranged from 2 ppm to 591 ppm Mo. The sample containing 591 ppm was from a quartz vein with visible molybdenite. This sample was collected from a prospect pit at the extreme northwest corner of the study area.

Zinc

Zinc is present in every sample that was analyzed. Sphalerite was most often observed in the breccia pipe as open space and replacement mineralization. It occurs in the stratigraphically higher parts of the breccia pipe.

It is evident that zinc was deposited outside and above the copper and gold deposition. Zinc shows spatial and temporal relationships with other base metals that are consistent with the predicted modes of transport and deposition.

Lead

Lead was detected in most of the geochemical samples from the study area. The highest value of 0.2 percent Pb was from a sample of moderately oxidized replacement ore.

The district wide metal zonation (Lovering, 1929) shows that most of the lead was deposited outside the study area, where lead and silver deposits are dominant. Pb and Ag were carried in solution further from the thermal source than Cu, Au, and Zn.

Cu-Mo-Au Relationship

Several recent studies of porphyry deposits have attempted to relate Cu, Mo and Au contents to plate tectonics and the petrologic processes that have resulted in the formation of these deposits (Kesler, 1972; Titley, 1978). The studies show that Cu-Au dominated deposits occur in island arc settings and are often associated with alkalic porphyry intrusives and coeval volcanic rocks. The most noteworthy of these deposits occur in the southwestern Pacific region and the Intermontana region of British Columbia, Canada. Cu-Mo dominated porphyries are most often associated with calc-alkalic porphyritic igneous rocks intruded into continental margins (southwestern United States). The huge porphyry deposit at Bingham Canyon, Utah, is an obvious exception since Cu, Au and Mo are all present in economic quantities.

Comparison of Cu, Mo and Au contents for the Alice E. and vicinity (Fig. 45) show that these are important constituents of the metallization.

The high gold values are the result of supergene enrichment of Cu-Au ores. It is apparent that a Cu-Au relationship and a Cu-Mo relationship exists. Au and Mo do not appear to be related.

The Alice E. system may be similar to Bingham Canyon, Utah with respect to copper, gold and molybdenum contents.

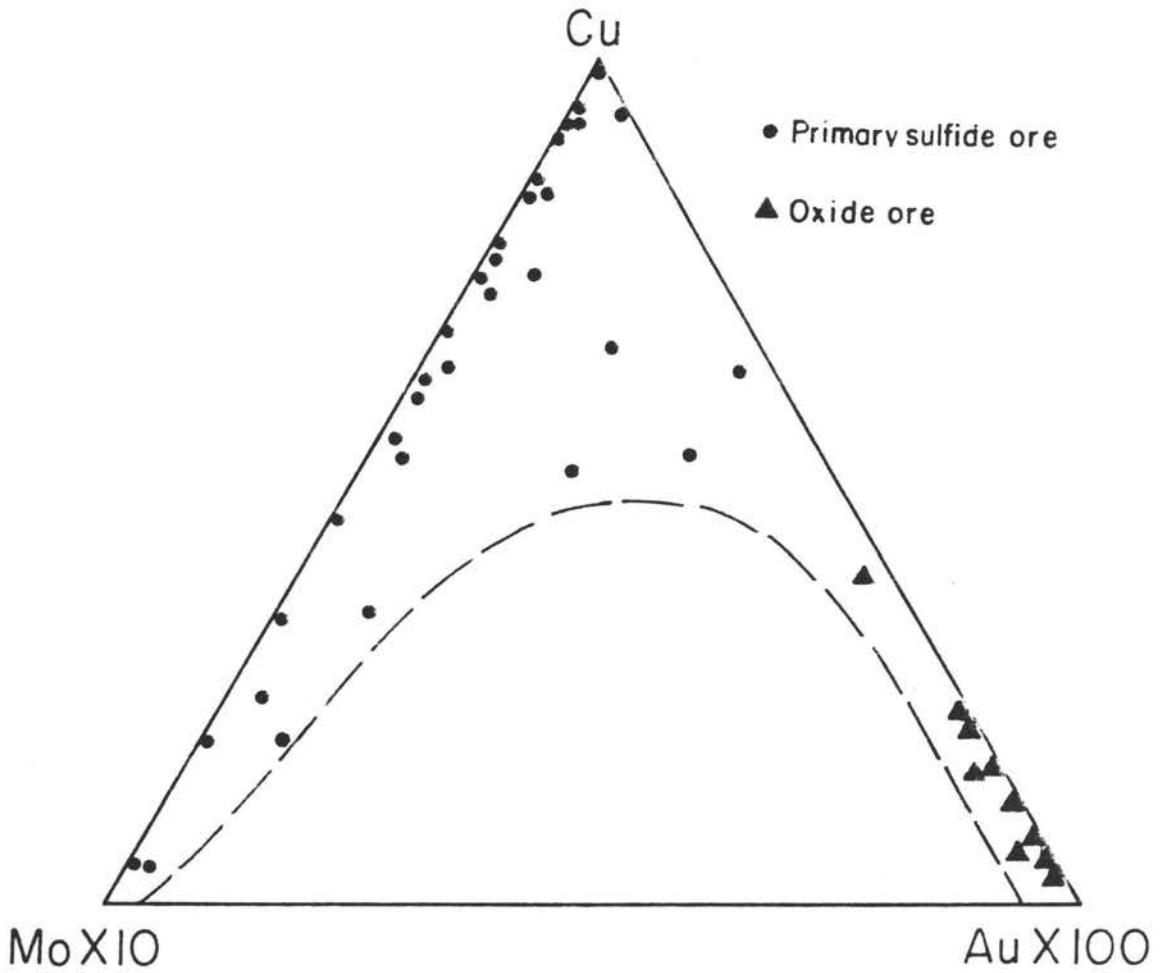


Figure 45. Plot of compositional data for 55 Alice E. samples.

DISCUSSION

Breccia Pipe Genesis

The Alice E. breccia pipe formed during a complex sequence of events that began approximately 55 m.y. ago. Geologists have argued for decades about the genesis of breccia pipes. The factual data available for the Alice E. breccia pipe do not clearly establish the origin of the pipe, but evidence suggests that two currently accepted mechanisms could be the source of brecciation within the area studied.

Withdrawal of magma from a high level volcanic reservoir would evacuate a portion of the magma chamber. Collapse of the magma chamber roof would follow with the development of a breccia column above the collapse zone. This theory is supported by Perry (1961), Kents (1964) and Bryner (1961). The features of the Alice E. breccia pipe suggest that this mechanism was at least partly responsible for the brecciation.

Evidence for this hypothesis lies mainly in the fact that all fragment movement in the pipe is downward and related to collapse. Angular fragments such as at the Alice E. are not characteristic of explosion type breccia pipes. Fragment rounding was not observed in the Alice E. breccia pipe indicating that a fluidized system did not develop at the level now exposed. The model assumes that brecciation penetrated the Cambrian rocks of the area but not into the rocks above since no lithologies younger than Cambrian age were discovered.

This early brecciation is intimately related to the intrusion of quartz amphibole latite porphyry dikes into the breccia pipe and the surrounding area. The dikes in the breccia pipe occur in a radial pattern (Plate 1) suggesting that a small stock may be present at depth in the breccia pipe.

Sheet and stockwork fracturing was created as the felsic intrusions were emplaced into the area. Resurgent boiling (Burnham, 1967) resulting from the evolution of vapor from a crystallizing magma (Whitney, 1975) could have provided the force ("hydraulic ramming") (Kents, 1964) for these types of fracturing.

Chemical brecciation (Sawkins, 1969) and mineralized stoping (Locke, 1926; Bryner, 1961) have provided little if any contribution to the brecciation. The mineralization clearly postdates the early brecciation in the Alice E. breccia pipe.

The breccia is a "collapse" breccia that has been created by intrusive and subsequent hydrothermal activity.

Controls of Mineralization

The mineralized areas of the Alice E. breccia pipe and vicinity can be related to physical and chemical controls which prevailed during the mineral deposition. A brief discussion of these physicochemical controls will help to define the nature of the mineralization.

Physical Controls

The formation of the breccia pipe and the many fractures that developed about the breccia pipe greatly increased the permeability of these rocks. Channelways were created through which metal-bearing fluids were able to pass freely upward and outward from some source

at depth. The breccia pipe may have provided access to the upper portions of a magma chamber and allowed the volatiles from the magma to rise unobstructed through the breccia. The breccia voids and veins in the vicinity were eventually filled with ore and gangue minerals deposited from the rising hydrothermal fluids.

The presence of thin-bedded limestones and shales has made these rocks particularly susceptible to replacement type mineralization. The breccia fragments of these rocks are in many places completely replaced by oxide and sulfide minerals. The thin beds provide high permeability along many bedding planes where replacement is initiated.

The breccia textures and fragment lithologies presently exposed show that brecciation extended upward into the Paleozoic sedimentary units but did not penetrate into the volcanic cover. It is apparent that venting of the system at the surface did not occur. Although highly permeable, the system was not truly open. This probably enhanced the potential for ore deposition within the pipe. A vented pipe would permit much more upward dispersion of the ore fluids with less chance for a significant deposit.

Chemical Controls

The fluid inclusion study established that gold was deposited with quartz and sulfides at temperatures exceeding 450°C and was still being deposited at temperatures as low as 320°C. It is evident from sampling that the highest grade gold occurs in veins and mineralized breccia whose fluid inclusion homogenization temperatures average 380°C. Most of the gold was deposited at temperatures below 400°C.

Halite-bearing inclusions and the high temperatures of ore deposition strongly suggest that the metals were carried in solution as chloride complexes. Helgeson and Garrels (1968) study of gold solubilities in aqueous chloride solutions indicate that gold is most likely transported as aurous chloride complexes (Au^+Cl_2^-) at elevated temperatures.

The ore mineral paragenesis can be adequately explained by the breakdown of metal chloride complexes due to cooling and dilution of the ore solutions. Mo, Cu, Au and Zn were deposited at progressively lower temperatures in the system. The stabilities of chloride complexes for the cations Cu^{2+} , Zn^{2+} , Pb^{2+} and Ag^+ are lowest for Cu^{2+} and highest for Ag^+ (Stanton, 1972, p. 153). This would explain the district metal zonation with Cu deposited in the center of the district and Ag peripheral to the Cu rich core. The stabilities of the metal complexes and the effect of cooling and dilution are important chemical controls of mineralization.

Studies of sulfide-oxide mineral stabilities (Barton et al., 1977) show that the activities of oxygen and sulfur in the aqueous phase will play an important role in determining the nature of mineral deposition. The Alice E. paragenesis indicates that a change from early oxide to later sulfide mineralization occurred.

Magnetite and chlorite were deposited due to an initially high a_{O_2} probably reflecting the nature of early fluids dominated by magmatic products. Extensive epidote-actinolite alteration accompanied the deposition of magnetite.

Sulfide mineralization followed the period of oxide mineralization by an unknown length of time. It is apparent that the a_{S_2} relative to

the a_{O_2} must have increased during this time. The reason for this is unknown but it is possible that as time progressed the input of sulfur from a source other than magmatic influenced the sulfur/oxygen ratios.

According to Helgeson and Garrels (1968), gold and pyrite will be deposited by a decrease in the oxidation state of the system. The change from magnetite to pyrite deposition at the Alice E. is accompanied by the deposition of gold as predicted from their calculations.

Sillitoe (1979) pointed out the fact that Au mineralization is often associated with magnetite in those porphyries where gold is important. Assuming that gold is carried as chloride complexes which at the Alice E. became unstable below 400°C, the a_{S_2} in the system may not be great enough to allow gold thio complexes (Seward, 1973) to form. The gold would be deposited along with a minor amount of Fe and Cu sulfides. In this manner gold could be concentrated in an area in close proximity to the igneous source. These factors are very important in the formation of a porphyry gold deposit.

Estimates of pH can be made based on the observed mineral assemblages. Alteration minerals such as actinolite, chlorite, epidote, sericite and carbonate all form in neutral to alkaline solutions. The lack of significant hypogene argillic alteration indicates that strongly acidic conditions were not developed in the Alice E. system. Since boiling occurred, it is possible that an argillic cap may have once existed at a level that has now been eroded from the system. The level now exposed is within the phyllic zone which commonly underlies an argillic and advanced argillic cap in porphyry deposits that are intact.

CONCLUSION AND RECOMMENDATIONS FOR FURTHER EXPLORATION

The Alice E. breccia pipe is a collapse breccia that contains zones of mineralization which are related to differentiated calc-alkalic intrusives (quartz amphibole latite porphyry). The mineralization consists of sulfides with gold in quartz veins, stockworks, and replacements of carbonate rocks. Mo, Cu and Au were deposited in the deeper higher temperature portions of the exposed deposits in and above a zone of boiling. Zn was deposited higher in the mineralized system at somewhat lower temperatures.

The deposit can be classified as Cu, Au, Zn deposit that has localized in a large subsidence breccia.

The most significant gold mineralization occurs in the sheet fractured zone at the Alice E. mine. It is evident that the mineralization was controlled in part by the level of boiling in the system. If the boiling occurred at the same elevation throughout the system, then ore might be deposited at similar elevations throughout the breccia pipe. The margins of the breccia pipe at the same elevation as the Alice E. would be the zones most likely to contain significant sheet fracture mineralization. The zone of gold mineralization at the Alice E. mine lies just at the southern edge of the breccia pipe. This is the lowermost exposed portion of the breccia pipe. The northern contact of the breccia is approximately 400 feet higher in elevation than the southern

contact. If the gold mineralization occurs at an elevation similar to that at the Alice E., the margins of the pipe could be tested for additional gold mineralization with drill holes of less than 500 feet in depth. The deepest drill holes would be required in the northern part of area where the depth to mineralization should be about 400 feet.

The area also warrants investigation for pervasive potassic zone mineralization at depth in the system. If the source of the surface mineralization is some larger system at depth, potential for a substantial porphyry deposit certainly exists. Deep drilling in excess of 1,000 feet would probably be required to test this possibility.

REFERENCES CITED

- Atkinson, W. W., Jr., 1975, Alteration and mineralization at Carr Fork, Bingham Mining District, Utah, *in* Guidebook of Bingham Mining District (Bray, R. E. and Wilsom, J. C., eds.): Soc. Econ.
- Bailey, E. H. and Stevens, R. E., 1960, Staining for potash and soda: *Amer. Mineralogist*, v. 45, p. 1020.
- Barr, D. A., and others, 1976, The alkaline suite porphyry deposits - a summary, *in* Porphyry deposits of the Canadian Cordillera (Sutherland-Brown, ed.): *Can. Inst. Min. and Metall.*, Special vol. 15, p. 359-367.
- Barton, P. B., Bethke, P. M. and Roedder, E., 1977, Environments of ore deposition in the Creede mining district, San Juan mountains, Colorado: Part III. Progress towards interpretation of the chemistry of the ore-forming fluid for the OH vein: *Econ. Geol.*, v. 72, no. 1, p. 1-24.
- Bryner, Leonid, 1961, Breccia and pebble columns associated with epigenetic ore deposits: *Econ. Geol.*, v. 56, p. 488-508.
- Burbank, W. S., 1941, Structural control of ore deposition in Red Mountain, Sneffels, and Telluride districts of the San Juan Mountains, Colorado: *Colo. Sci. Soc. Proceed.*, v. 14, p. 141-261.
- Burnham, C. W., 1967, Hydrothermal fluids at the magnatic stage, *in* *Geochemistry of hydrothermal ore deposits*, (H.L. Barnes, ed.): New York, Holt, Rinehart and Winston, Inc., 670 p.
- Burnham, C. W. and Ohmoto, H., 1980, Late stage processes of felsic magnetism, *in* *Granite magmatism and related mineralization* (Ishihara, S. and Takenouchi, S., eds): *Soc. of Mining Geologists of Japan, Mining Geology Special Issue*, No. 8, 11 p.
- Butler, T. A., 1965, Republic mines and vicinity, New World mining district, Montana and Wyoming: unpublished M.S. thesis, University of Idaho.
- Carlson, S. R. and Sawkins, F. J., 1980, Mineralogic and fluid inclusion studies of the Tourmalina Cu-Mo-bearing breccia pipe, northern Peru: *Econ. Geol.* v. 75, no. 8, p. 1233-1238.
- Chadwick, R. A., 1970, Belts of eruptive centers in the Absaroka-Gallatin volcanic province: *Geol. Soc. of America Bulletin*, v. 81, p. 267-274.

- Cope, E. L., 1981, Characteristics of porphyry gold deposits: unpublished Energy Reserves Group Inc. report, 35 p.
- Creasy, S. C., 1966, Hydrothermal alteration, in *Geology of the porphyry copper deposits, Southwestern North America* (Titley, S. R. and Hicks, C. L., eds.): The Univ. Arizona Press, Tucson, p. 51-74.
- Cunningham, C. G., 1978, Pressure gradients and boiling as mechanisms for localizing ore in porphyry systems: *Jour. Research U.S.G.S.*, v. 6, no. 8, p. 745-754.
- Dickenson, W. R. and Snyder, W. S., 1979, Geometry of triple junctions and subducted slabs related to San Andreas transform: *Jour. Geophys. Res.* 84, p. 561-672.
- Einaudi, M. T., 1982, Terminology, classification and composition of skarn deposits: *Econ. Geol.*, v. 77, no. 4, p. 745-754.
- Elliott, J. E., 1979, Geologic map of the southwest part of the Cooke City quadrangle: U.S.G.S. Map I-1084.
- Erwood, R. J., Kesler, S. E. and Cloke, P. L., 1979, Compositionally distinct, saline hydrothermal solutions, Naica mine, Chihuahua, Mexico: *Econ. Geol.*, v. 74, no. 1, p. 95-108.
- Eyrich, H. T., 1969, Economic geology of part of the New World mining district, Park County, Montana: unpublished Ph.D. dissertation, Washington State University.
- Foose, R. M., Wise, D. W. and Garbarini, G. S., 1961, Structural geology of the Beartooth mountains, Montana and Wyoming: *Geol. Soc. of Amer. Bulletin*, v. 72, p. 1143-1172.
- Hague, A., 1899, Description of the Absaroka quadrangle: U.S. Geol. Survey Geol. Atlas, Folio 52.
- Helgeson, H. C. and Garrels, R. M., 1968, Hydrothermal transport and deposition of gold: *Econ. Geol.*, v. 63, p. 622-635.
- Hemley, J. J. and Jones, W. R., 1964, Chemical aspects of hydrothermal alteration with emphasis on hydrogen metasomatism: *Econ. Geol.*, v. 59, no. 4, p. 538-569.
- Horral, K. B., 1966, The petrology of the Henderson Mountain laccolith, Park County, Montana: unpublished M.S. thesis, Northern Illinois University.
- Iddings, J. P., 1895, Absarokite-shoshonite-banakite-series: *Jour. of Geol.*, v. 3, p. 935-959.
- Jansons, U. J., 1963, Petrography, petrology and trace element relations of the Cooke City (Montana) porphyry, unpublished M.S. thesis, Montana State University, 58 p.

- Joplin, G. A., 1968, The shoshonite association - A review: *Geol. Soc. Australia Jour.*, v. 15, p. 275-294.
- Lange, I. M., 1977, Map of metallic mineral deposits of western Montana: Montana Bureau of Mines and Geology openfile report 29.
- Lanier, G., Folsom, R. B. and Cone, S., 1975, Alteration of equigranular quartz monzonite Bingham Mining district, Utah, in *Guidebook to the Bingham mining district* (Bray, R. E. and Wilson, J. C., eds.): *Soc. Econ. Geologists Field Conf.*, p. 73-97.
- Lipman, P. W., Christiansen, R. L. and Prostka, H. J., 1972, Cenozoic volcanism and plate-tectonic evolution of the western United States: 1. Early and middle cenozoic: *Phil. Trans. Roy. Soc. London* 271, p. 217-248.
- Lipman, P. W., 1980, Cenozoic volcanism in the western United States: Implications for continental tectonics: *Studies in geophysics*, National Academy of Sciences, Washington, D.C., p. 161-174.
- Locke, A., 1926, The formation of certain orebodies by mineralization stoping: *Econ. Geol.*, v. 21, p. 531-543.
- Lovering, T. S., 1929, The New World or Cooke City mining district, Park County, Montana: *U.S. Geol. Survey Bull.* 911-A, p. 1-87.
- Lowell, D. G. and Guilbert, J. M., 1970, Lateral and vertical alteration-mineralization zoning in porphyry ore deposits: *Econ. Geol.*, v. 65, no. 4, p. 373-408.
- Meinhert, L. D., 1982, Skarn, manto and breccia pipe formation in sedimentary rocks of the Cananea mining district, Sonora, Mexico: *Econ. Geol.*, v. 77, no. 4, p. 919-949.
- Nash, J. T., 1976, Fluid inclusion petrology-data from porphyry copper deposits and applications to exploration: *U.S. Geol. Survey Prof. Paper* 907-D, 16 p.
- Parson, W. H., 1939, Volcanic centers in the Sunlight area, Park County, Wyoming: *Jour. Geol.*, v. 47, p. 1-26.
- Perry, V. D., 1961, The significance of mineralized breccia pipes: *Min. Eng.*, v. 10, no. 2, p. 367-376.
- Peterman, Z. E., Doe, B. R. and Prostka, H. J., 1970, Lead and strontium isotopes in rocks of the Absaroka volcanic field, Wyoming: *Contr. Mineralogy and Petrology*, v. 27, p. 121-130.
- Prostka, H. J., 1972, Hybrid origin of the Absarokite-shoshonite-banakite series, Absaroka volcanic field, Wyoming: *Geol. Soc. Amer. Bull.*, v. 84, p. 687-702.

- Reed, G. C., 1950, Mines and mineral deposits (except fuels), Park County, Montana: U.S. Bur. Mines Inf. Circ. 7546, 68 p.
- Reid, J., 1975, Skarn alteration of the Commercial Limestone in the Carr Fork area, in Guidebook of Bingham mining district (Bray, R. E. and Wilson, J. C., eds.): Soc. Econ. Geol. Field Conf., p. 105-118.
- Rose, A. W., 1970, Zonal relations of wallrock alteration and sulfide distribution at porphyry copper deposits: *Econ. Geol.*, v. 65, no. 8, p. 920-936.
- Rose, A. W. and Burt, D. M., 1979, Hydrothermal alteration, in Geochemistry of hydrothermal ore deposits, 2nd ed: Wiley and Sons, New York, p. 173-235.
- Rouse, J. T., 1937, Genesis and structural relations of the Absaroka volcanic rocks: *Geol. Soc. Amer. Bull.*, v. 48, p. 1257-1296.
- Sawkins, F. J., 1969, Chemical brecciation, an unrecognized mechanism for breccia formation?: *Econ. Geol.*, v. 64, p. 613-617.
- Seward, T. M., 1973, Thio complexes of gold and the transport of gold in hydrothermal ore solutions: *Geochim. Cosmochim. Acta*, v. 37, p. 379-399.
- Sillitoe, R. H. and Sawkins, F. J., 1971, Geologic, mineralogic and fluid inclusion studies relating to the origin of copper-bearing tourmaline breccia pipes, Chile: *Econ. Geol.*, v. 66, p. 1028-1041.
- Sillitoe, R. H., 1979, Some thoughts on gold rich porphyry deposits: *Mineralium Deposita*, v. 14, p. 161-174.
- Smedes, H. W. and Prostka, H. J., 1972, Stratigraphic framework of the Absaroka Volcanic Supergroup in the Yellowstone National Park region: U.S. Geol. Survey Prof. Paper 729-C, 33 p.
- Stanton, R. L., 1972, Ore petrology, McGraw-Hill, New York, 713 p.
- Streckeisen, A., 1979, Classification and nomenclature of volcanic rocks, lamprophyres, carbonatites, and melilitic rocks: Recommendations and suggestions of the IUGS Subcommittee on the Systematics of Igneous rocks, 5 p.
- Stringham, B., 1952, Fields of formation of some common hydrothermal-alteration minerals: *Econ. Geol.*, v. 47, no. 6, p. 661-664.
- Thompson, T. B., 1968, Hydrothermal alteration and mineralization of the Rialto Stock, Lincoln County, New Mexico: *Econ. Geol.*, v. 63, no. 8, p. 943-949.
- Westra, G., and Keith, S. B., 1981, Classification and genesis of stockwork molybdenum deposits: *Econ. Geol.*, v. 76, no. 4, p. 844-873.

Whitney, J. A., 1975, Vapor generation in a quartz monzonite magma:
A synthetic model with application to porphyry copper deposits:
Econ. Geol., v. 70, no. 2, p. 346-358.

APPENDIX

Table 7. Geochemical data for 55 Alice E. samples. All values in parts per million unless otherwise noted.

Sample	Au	Ag	Cu	Mo	Zn	Pb	Te
CC-81-1	4.52	34.1	300	2	200	59	69
81-2	1.95	9.8	70	--	28	22	81
81-3	0.16	1.6	38	2	10	7	--
81-4	2.06	9.0	15	--	15	--	7
81-5	0.20	4.0	260	--	46	12	*
81-6	1.01	6.5	15	--	14	149	*
81-7	0.58	5.1	12	--	14	73	*
81-8	2.65	8.4	11	--	16	69	*
81-9	5.36	10.8	87	2	11	5	*
81-10	1.66	0.5	47	--	1	2	*
81-11	--	4.5	250	--	44	32	*
81-12	--	1.2	69	--	34	15	*
81-13	--	1.7	172	2	50	5	*
81-14	--	1.2	96	--	22	11	*
81-15	--	4.9	470	3	168	167	*
81-16	--	2.0	26	3	8	2	*
81-17	--	2.0	390	--	98	14	*
81-18	--	2.3	170	--	157	68	*
81-19	--	19.3	750	10	460	1540	*
81-20	--	3.0	300	--	66	28	*
81-21	0.17	5.2	310	2	38	98	*
81-22	2.02	10.2	10	--	13	42	*
81-23	1.97	90.0	74	4	33	168	*

-- element not detected

* element not analysed

Table 7. Continued.

Sample	Au	Ag	Cu	Mo	Zn	Pb	Te
CC-81-24	6.06	143.0	20	3	26	88	76
81-25	0.20	5.0	28	--	17	33	2
81-26	0.94	11.3	58	2	100	42	127
81-27	0.48	8.2	118	--	82	21	60
81-28	10.58	8.6	35	4	27	158	12
81-29	0.68	3.1	109	3	24	10	6
81-30	0.03	1.3	320	64	17	4	1
81-31	0.20	2.4	360	--	84	22	2
81-32	0.51	2.8	600	45	34	5	2
82-6	0.03	4.0	324	591	148	62	*
82-15	0.04	--	172	68	87	68	*
82-17	0.03	--	17	24	31	32	*
82-35	0.09	1.0	464	31	4.42%	165	*
82-40	0.07	--	668	22	405	130	*
82-41	0.09	--	30	5	309	51	*
82-42	0.03	--	21	6	48	40	*
82-43	0.05	--	434	3	177	43	*
82-46	0.03	--	315	3	207	62	*
82-50	0.66	4.0	823	21	217	0.21%	*
82-52	1.16	3.0	415	9	60	21	*
82-53	0.04	--	90	7	87	32	*
82-54	0.05	1.0	354	6	69	68	*
82-55	0.01	--	131	6	116	79	*
82-56	0.37	--	92	33	105	292	*
82-61	0.01	--	11	13	55	121	*

Table 7. Continued.

Sample	Au	Ag	Cu	Mo	Zn	Pb	Te
CC-82-62	0.03	--	186	11	64	82	*
82-63	0.02	--	388	7	50	66	*
82-64	0.03	--	716	19	60	57	*
82-65	0.06	--	0.125%	4	62	39	*
82-66	0.03	--	132	5	115	55	*
82-67	0.02	--	210	6	98	61	*
82-68	0.04	--	78	4	87	49	*

Semi-Quantative Method of Determining
Quartz Contents of Porphyritic
Aphanitic Rocks Using
X-Ray Diffraction

Edward L. Cope
Department of Earth Resources
April 15, 1983

Introduction

A method for determining the quartz contents of porphyritic rocks with an extremely fine grained groundmass (0.01 mm) was used to aid in obtaining modal data necessary to classify the igneous rocks. The staining of cut specimens aided greatly in estimating groundmass compositions of most of the rocks, but several samples were difficult to determine. These samples were selected for analysis. The method used here was recommended by Dr. L. K. Burns, Colorado State Earth Resources Department.

Sample Preparation

The samples of porphyry were crushed and separates of the light minerals were prepared by extracting the minor magnetite and mafic minerals by magnetic isodynamic separation methods on a Frantz magnetic separator. The light mineral separates were then powdered and applied to standard glass slides using acetone.

Preparation of Standard Samples

Standard synthetic rock types were prepared by combining appropriate rock type weight percent quantities of quartz, orthoclase

and oligoclase. The mineral samples were obtained from the Colorado State Earth Resources Department mineral collection. The minerals were powdered and the synthetic rock type were weighed out on the analytical balance. The rock standards were created according to the weights of each mineral as shown in Table 8.

Table 8. Quartz, orthoclase and oligoclase contents of synthetic rock standards.

	Latite		Rhyodacite	
	wt. %	grams	wt. %	grams
Quartz	2	0.01	25	0.125
Orthoclase	49	0.245	37.5	0.1875
Oligoclase	49	0.245	37.5	0.1875
	100	0.5	100	0.5

The standard samples were mixed thoroughly and applied in the same manner as the unknown samples to glass slides with acetone.

X-Ray Procedure

The samples were run on a General Electric X-ray diffraction machine using $K\alpha$ radiation. The samples were started at $6^\circ 2\theta$ and run to $65^\circ 2\theta$ at a speed of $2^\circ 2\theta$ per minute.

Assimilation of Data

The X-ray diffraction patterns obtained from the standards and unknowns were studied to isolate and select a quartz peak that could be used for comparison purposes in all of the samples. The 60°

2 θ peak was chosen and the area under this peak was measured for each X-ray diffraction pattern. The areas were determined using an electronic planimeter and recorded in square inches. The results are presented in Table 9.

Table 9. Data obtained by measuring the area under the 60° 2 θ quartz peaks from X-ray diffraction patterns.

Sample	Area Inches ²
Standard Latite	0.005
Standard Rhyodacite	0.043
CC-82-9	0.009
CC-82-45	0.037
CC-82-68	0.069

Graphic representation of the data (Fig. 46) allows determination of quartz contents of the unknowns by comparison or ratioing them against the standards. The weight percentage of quartz in the three unknown samples is presented in Table 10.

Table 10. Weight percent quartz for three Alice E. samples.

Sample	wt. % Quartz
CC-82-9	3.5
CC-82-45	21.5
CC-82-68	41.0

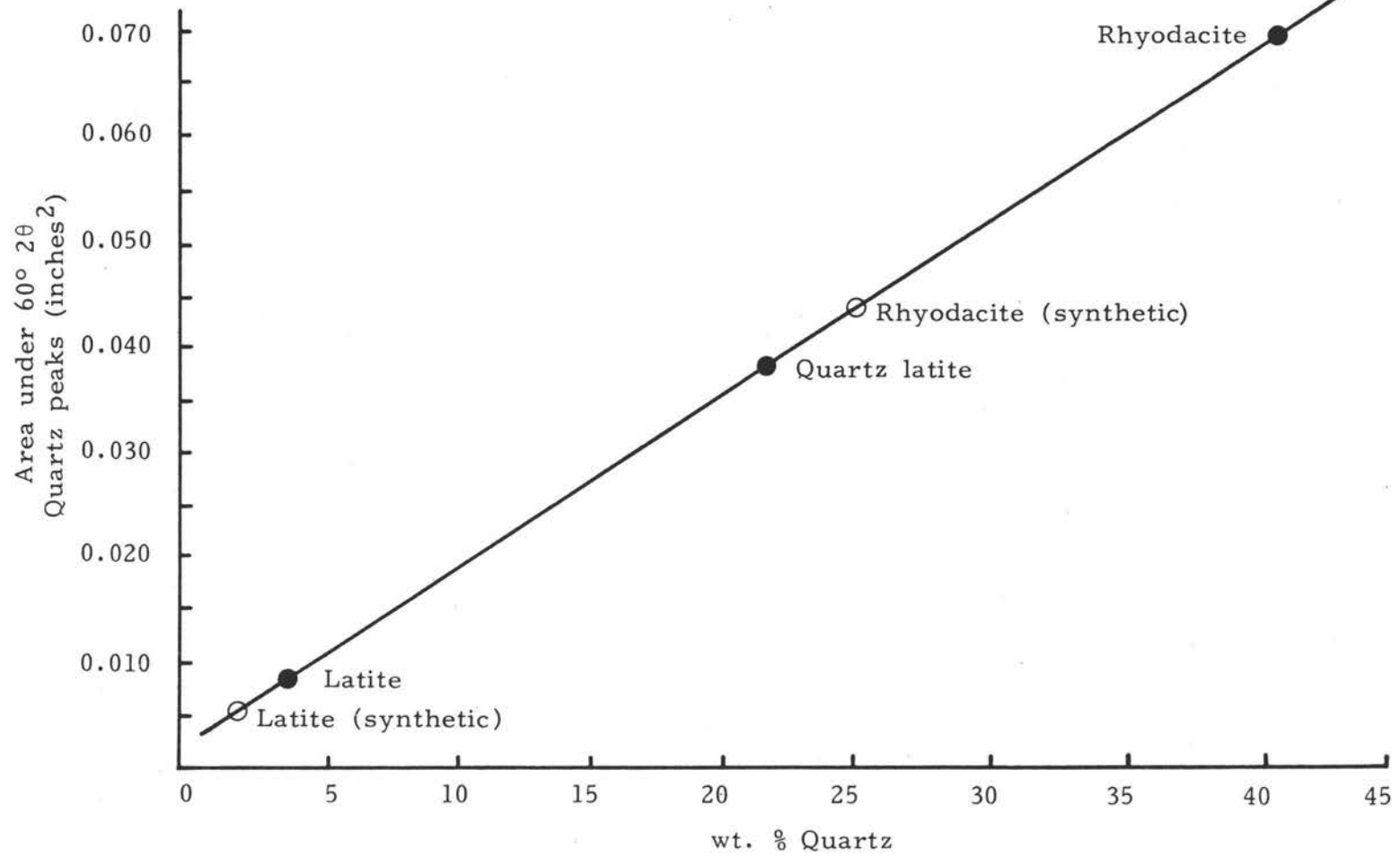


Figure 46. Graphic representation of X-ray diffraction data.

The densities of the three minerals quartz, orthoclase, and oligoclase are similar, allowing direct conversion from weight percent mineral compositions to volume percent composition. The volume percent quartz was used in determining the modes of the porphyries that presented classification problems.

Table 11. Heating stage data for primary fluid inclusions in quartz related to sulfide-gold mineralization at the Alice E. mine and vicinity.

Sample	Inclusion Type	Filling Temp. Trials (°C)			Mean Filling Temp. (°C)	Halite Dissolution (°C)
		1	2	3		
CC-82-1	III	357	360	359	359	-
	I	330	324	328	327	-
	I	353	354	356	354	-
	I	373	372	369	371	-
	I	373	372	369	371	-
	III	380	383	-	382	-
	I	350	351	-	351	-
	I	353	352	351	352	-
	I	363	364	361	363	-
	I	373	374	372	373	-
	I	385	386	385	385	-
	I	357?	354	354	354	-
	I	425	426	427	426	-
	III	307	408	407	407	180
	III	380	380	380	380	187
	I	398?	401?	395	395	-
	I	391	389	389	389	-
	I	380	380	380	380	-
	I	418?	415	-	415	-
	CC-82-52	I	422	422	420	422
I		372	373	372	372	-
III		358	360	360	360	250

Table 11. Continued.

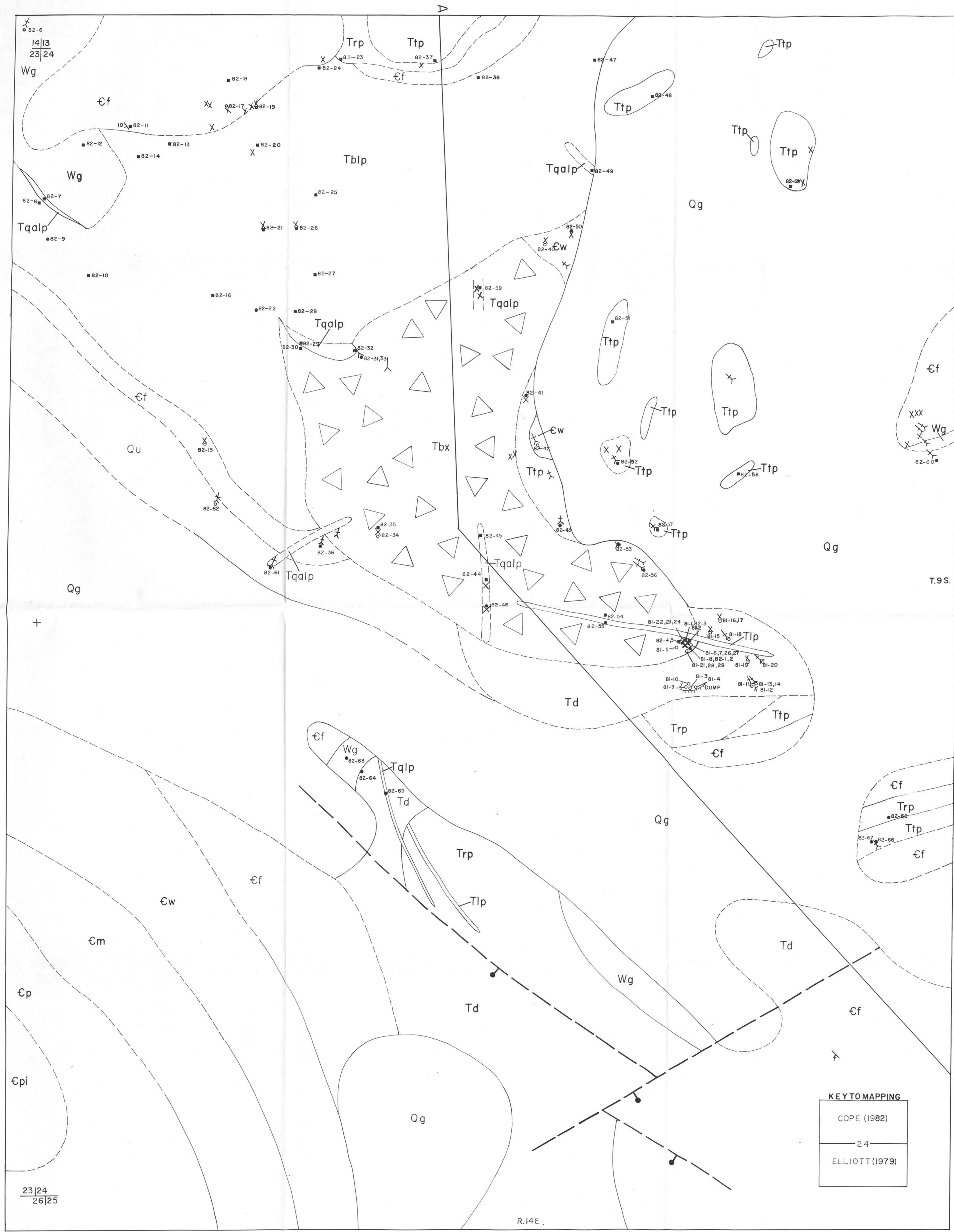
Sample	Inclusion Type	Filling Temp. Trials (°C)			Mean Filling Temp. (°C)	Halite Dissolution (°C)
		1	2	3		
CC-82-53	I	360	357	357	357	-
	I	345	342	338	342	-
	I	430	430	431	430	-
	I	446	449?	446	446	-
	I	358	358	358	358	-
	III	472	469	472	470	+500
	I	398	399	400	399	-
	I	351	352	-	352	-
	III	421	419	418	419	-
	I	353	353	354	353	-
	III	369	371	369	370	-
CC-82-60	I	385	383	386	385	-
	I	295	296	296	296	-
	I	319	320	319	320	-
	I	321	321	321	321	-
	I	319	318	319	319	-
CC-82-63	I	493	497	-	495	-
	II	+530	-	-	?	-
	I	443	447	449	447	-
	I	520	519	-	520	-
	I	465	-	-	465	-

MAP UNITS

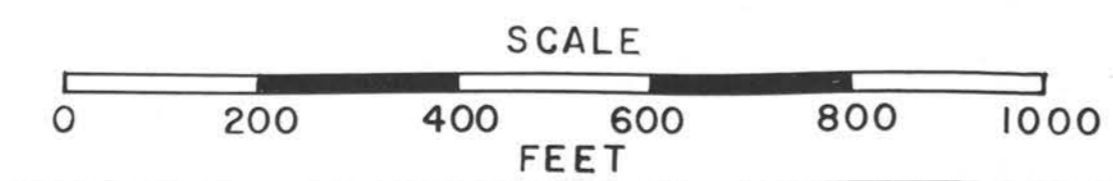
- Qu UNDIFFERENTIATED ALLUVIUM (HOLOCENE)
- Qg GLACIAL DEPOSITS (PLEISTOCENE)
- Tqalp QUARTZ LATITE PORPHYRY (EOCENE)
- Tql LATITE PORPHYRY (EOCENE)
- Tqalp QUARTZ AMPHIBOLE LATITE PORPHYRY (EOCENE)
- Tbtp BIOTITE LATITE PORPHYRY (EOCENE)
- Tbx ALICE E. BRECCIA PIPE (EOCENE)
- Trp RHYODACITE PORPHYRY (PALEOCENE)
- Td DIORITE (PALEOCENE)
- Ttp TRACHYANDESITE PORPHYRY (PALEOCENE)
- €pi PILGRIM LIMESTONE (UPPER CAMBRIAN)
- €p PARK SHALE (MIDDLE CAMBRIAN)
- €m MEAGHER LIMESTONE (MIDDLE CAMBRIAN)
- €w WOLSEY SHALE (MIDDLE CAMBRIAN)
- €f FLATHEAD SANDSTONE (MIDDLE CAMBRIAN)
- Wg GRANITIC GNEISS (PRECAMBRIAN W)

SYMBOLS

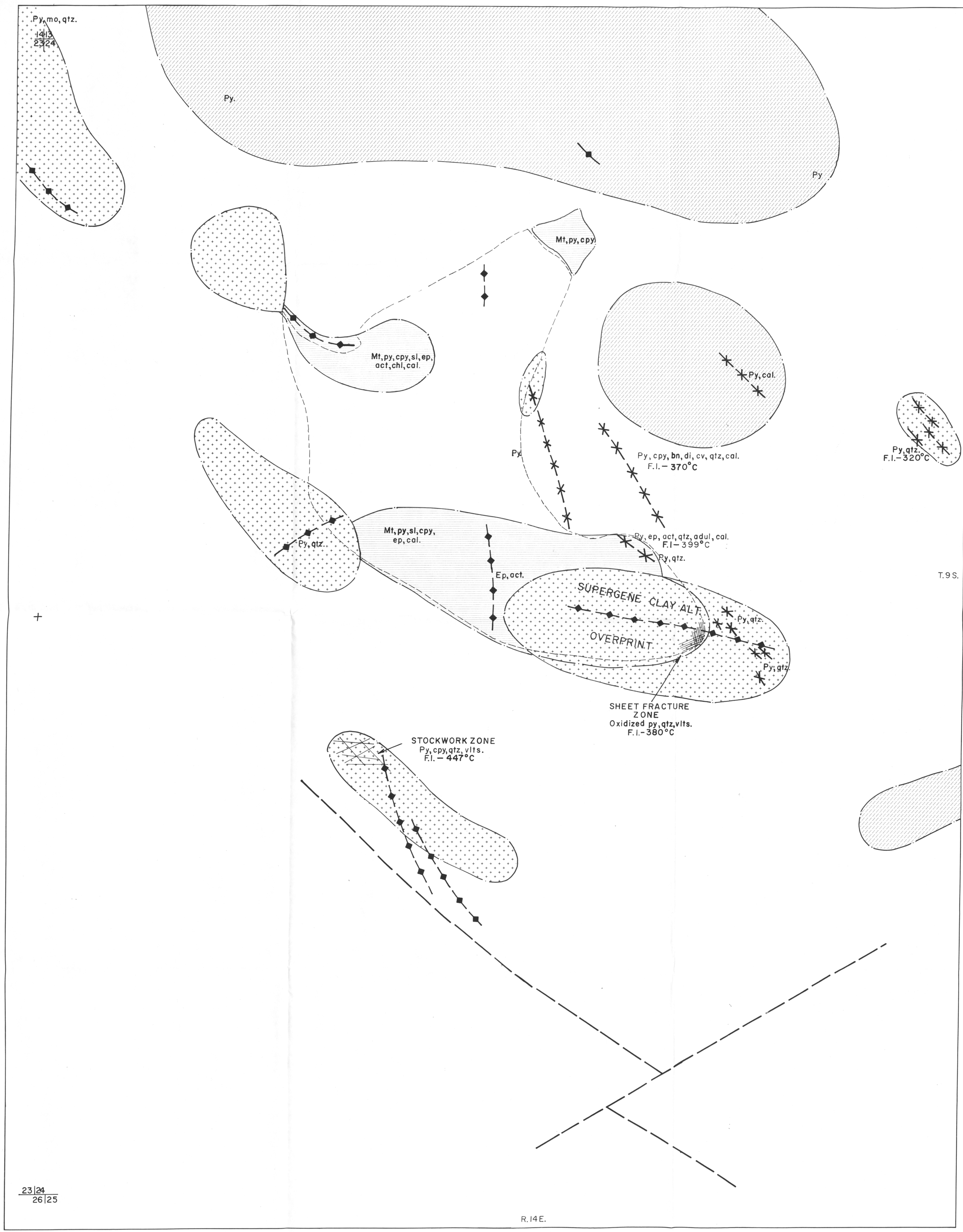
- CONTACT—Dashed where approximately located.
- FAULT—Bar and ball on downthrown side.
- STRIKE AND DIP OF INCLINED BEDS
- ALICE E. MINE
- CAVED ADIT
- PROSPECT PIT
- SAMPLE LOCATION—Geochemical, petrographic, both types




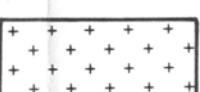
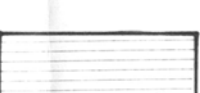
KEY TO MAPPING
 COPE (1982)
 — 2.4 —
 ELLIOTT (1979)



ALICE E. BRECCIA PIPE				
GEOLOGY				
SEC. 24	T. 9S.	R. 14E.	SCALE 1" = 200'	BY EDWARD L. COPE
COUNTY PARK	STATE MT			








ALTERATION TYPES

-  PROPYLITIC
-  PHYLIC
-  SKARN ALTERATION

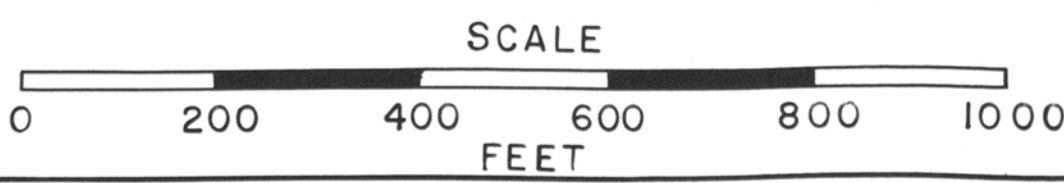
ABBREVIATIONS

- mt MAGNETITE
- py PYRITE
- mo MOLYBDENITE
- cpy CHALCOPYRITE
- bn BORNITE
- sl SPHALERITE
- ep EPIDOTE
- act ACTINOLITE
- chl CHLORITE
- qtz QUARTZ
- adul ADULARIA
- cal CALCITE
- F.I. FLUID INCLUSION HOMOGENIZATION TEMPERATURE

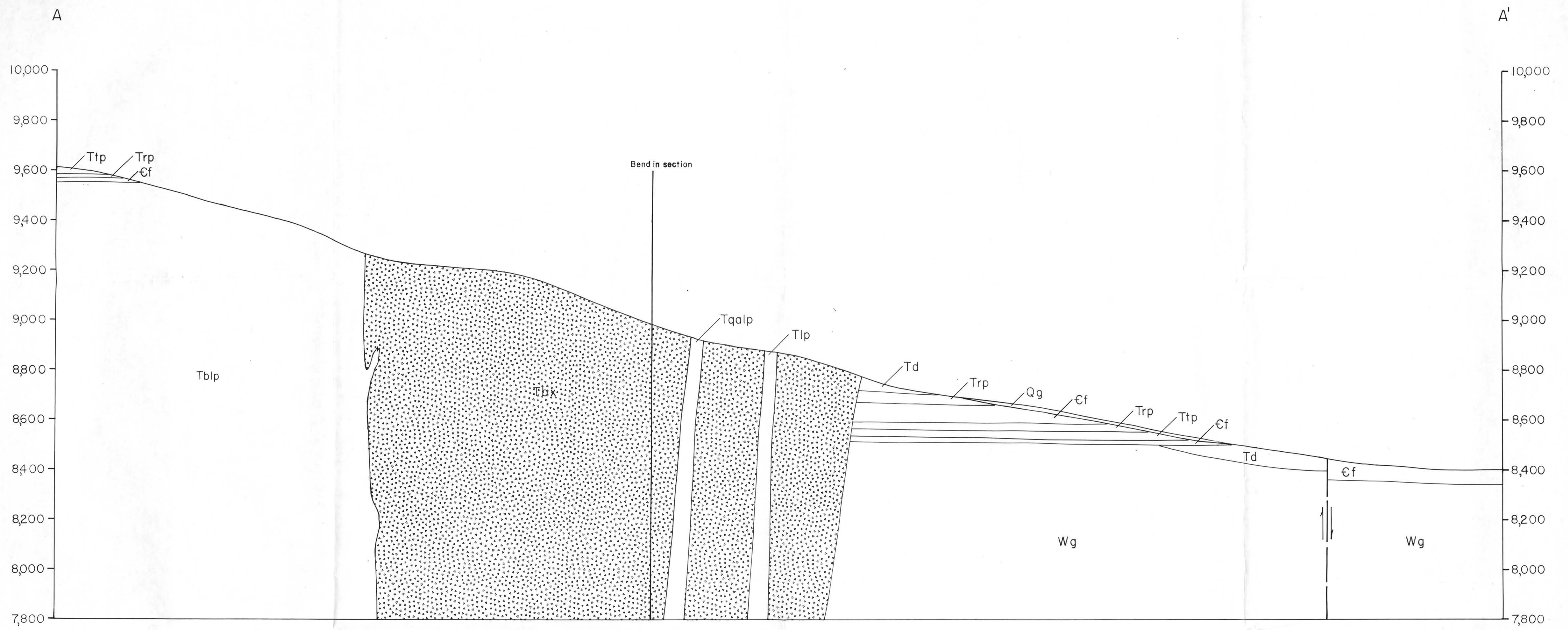
SYMBOLS

-  OUTLINE OF BRECCIA PIPE
-  ALTERATION CONTACT
-  FAULT
-  DIKE
-  VEIN

23/24
26/25



ALICE E. BRECCIA PIPE			
ALTERATION - MINERALIZATION			
SEC. 24	T. 9S.	R. 14E.	SCALE 1" = 200'
COUNTY PARK	STATE MT	BY EDWARD L. COPE	



GEOLOGIC CROSS SECTION
 A-A'
 ALICE E. BRECCIA PIPE
 See Geologic Map (Plate I) for explanation of symbols.
 SCALE
 0 200 400 600 800 1000
 FEET
 BY
 EDWARD L. COPE